12 November 2021

Dear Editors,

Re: AGEO: Your Submission - [EMID:6b810a73f1b0eee4]

Thank you for the reviews of our manuscript and for the opportunity to address the issues raised by the reviewers. We have amended the text of the manuscript in line with both the reviewers' comments and provide a step-by-step response to these comments below.

Yours sincerely,

Yuze Wang,

On behalf of our co-authors

Responses to reviewers' comments

Reply to Reviewer #1:

Reviewer #1's general comments: This manuscript is interesting as the authors optimized the MICP process by bridging microscale and macroscale tests. The main finding of this study is that longer injection intervals could effectively enhance the improvement of strength. The major concern of this research is the distinct materials used in microscale test, i.e. PDMS, and macroscale test, i.e. silicon sands. This difference may lead to different crystallization behaviors. Another issue is that the text of literature review is short with limited citations while that of results is a little long, especially in microscale experiments. The reviewer is noted that some of descriptions in results sections, such as protocol 1 and 2, seem to be overlapped.

Reply: We appreciate that Reviewer #1 found this manuscript interesting and Reviewer #1's comments for us to improve this manuscript. Reviewer #1's general comments are divided into three parts and the revisions are as below:

Yuze Wang, Assistant Professor, PhD, Department of Ocean Science and Engineering, Southern University of Science and Technology, Shenzhen, People's Republic of China (corresponding author). E-mail: wangyz@sustech.edu.cn

#C1. *The major concern of this research is the distinct materials used in microscale test, i.e. PDMS, and macroscale test, i.e. silicon sands. This difference may lead to different crystallization behaviors.*

#R1： The contents in lines 97-104 in the original version of the manuscript were changed into the contents as bellow (see Lines 104-110 in the revised version of the manuscript):

> **"**However, the porous media in microfluidic chips are normally two-dimensional structures with the third dimension having the same thickness made using polydimethylsiloxane (PDMS), which do not fully replicate the three-dimensional features and surface properties of the porous media of soils such as silicon sands. Therefore, the optimized protocols obtained using microfluidic and soil column experimental methods may be different. Since there are not any previous studies that explore the link between these two types of experiments, the primary objective of this study is to compare the similarities and differences between the optimized MICP protocols at the two scales."

#C2. Another issue is that the text of literature review is short with limited citations while that of results is a little long, especially in microscale experiments.

#R2. Literature review was extended (see Lines 68-102 in the revised version of the manuscript):

> "Compared to traditional cement, the biofluids which are injected into soil pores or rock fractures have lower viscosities enabling their injection over larger distances, as well as their penetration into smaller fractures. In addition, $CaCO_3$ is also more environmentally friendly compared to cement. However, there are still challenges to overcome before MICP can be widely used in real engineering applications. The bio-geo-chemical processes involved in this technique are complex, making it challenging to control and predict the engineering performance of MICP-treated soils at the macro-scale, especially under real environmental conditions. For engineering applications, MICP treatment efficiency needs to be improved significantly in order to become economically viable. Studies have shown that effectiveness of MICP for soil strength enhancement is affected by properties of $CaCO_3$ crystals and the chemical transformation efficiency, the latter of which affects the calcium carbonate content in treated soils (Al Qabany et al., 2012, Al Qabany & Soga, 2013, Cheng et al., 2017).

Yuze Wang, Assistant Professor, PhD, Department of Ocean Science and Engineering, Southern University of Science and Technology, Shenzhen, People's Republic of China (corresponding author). E-mail: wangyz@sustech.edu.cn

To overcome the challenges, experimental studies have been conducted to understand the process of MICP and to optimize the treatment protocols. In addition, numerical simulations on MICP have also been developed to link the experiments of MICP to field scale MICP performance. Soil column experiments, which combine carbonate content testing, unconfined compressive strength testing and/or scanning electron microscopy imaging, have been widely conducted as one of the main methods used for studying MICP. The factors and experimental conditions affecting MICP that have been studied include saturation of soil samples (Cheng & Cord-Ruwisch, 2012), bacterial density, reaction time and curing condition (Zhao et al., 2014), particle size distribution (Mahawish et al., 2018), pH (Cui et al. 2020), and concentration of cementation solution (Zhao et al., 2014; Lai et al., 2021).

In recent years, microfluidic chip experiments, have become popular for studying the microscale properties of MICP due to the fact that the *in-situ* behaviour of bacteria and calcium carbonate during MICP treatment can be observed and investigated (Wang et al., 2019a). A microfluidic chip enables the manipulation of small amounts of fluid (Whitesides, 2006) and can replicate key features of the porous matrix of sandy soil such as the shape irregularity of sand grains and pores, as well as the surface properties of the porous channel (Wang et al., 2019a). By performing microfluidic chip experiments, MICP has been further explored in terms of microscale processes (Wang et al.2019b; Kim et al. 2020), MICP precipitation kinetics (Kim et al. 2020; Wang et al. 2021; Xiao et al. 2021), micro-scale changes with pH variations during MICP treatment (Zehner et al., 2020), and the role of bacteria in MICP and its effects on MICP processes and kinetics (Wang et al. 2021). In addition, microfluidic chip experiments have also been used for studying EICP (Kim et al. 2020, Zehner et al. 2021, Weinhardt et al. 2021). Unlike core scale or model scale soil experiments, microfluidic chip experiments are capable of observing bacterial behaviour and monitoring the whole precipitation processes of calcium carbonate in the porous medium under conditions that mimic the flow conditions in the soil matrix. This provides an opportunity to further explore the microscale mechanisms of MICP or EICP, which will help to advance the understanding the of engineering behaviours of MICP-treated soils."

In addition, results of microfluidic chip experiments were shortened by delating the not essential

Yuze Wang, Assistant Professor, PhD, Department of Ocean Science and Engineering, Southern University of Science and Technology, Shenzhen, People's Republic of China (corresponding author). E-mail: wangyz@sustech.edu.cn

figures and relative context. The figures now for microfluidic number is reduced from 9 to 7 (Please see the revised Section 3.1, 3.2, 3.3 and 4.1 for the microfluidic chip results in the revised version of the manuscript).

#C3. The reviewer is noted that some of descriptions in results sections, such as protocol 1 and 2, seem to be overlapped.

R3. To distinguish the protocol names, the number of the microfluidic chip experiment were numbered as M1, M2, M3 and M4, soil column experiments were numbered as S1-S9 in Tables 1 and 2, respectively. The results of microfluidic chip experiments were heavily revised to become clearer. In addition, to avoid overlap of the results description, results and discussion are separated into two separate sections (please see Section 3.1, 3.2 and 4.1 in the revised manuscript).

Reviewer #1's detailed comments and the revisions are as below:

C1. L98-104. The novelty of this study is needed to be addressed in detail. More recent references about microfluidics in MICP are supposed to be summarized, such as: "Using microfluidic set-up to determine the adsorption rate of sporosarcina pasteurii bacteria on sandstone."; "Assessing the kinetics and pore-scale characteristics of biological calcium carbonate precipitation in porous media using a microfluidic chip experiment."; "Kinetic biomineralization through microfluidic chip tests."

R1: A paragraph was added to summarize the recent references about microfluidics in MICP as below (see Lines 88-102 in the revised version of the manuscript):

> "In recent years, microfluidic chip experiments, have become popular for studying the microscale properties of MICP due to the fact that the *in-situ* behaviour of bacteria and calcium carbonate during MICP treatment can be observed and investigated (Wang et al., 2019a). A microfluidic chip enables the manipulation of small amounts of fluid (Whitesides, 2006) and can replicate key features of the porous matrix of sandy soil such as the shape irregularity of sand grains and pores, as well as the surface properties of the porous channel (Wang et al., 2019a). By performing microfluidic chip experiments, MICP has been further explored in terms of microscale processes (Wang et al.2019b; Kim et al. 2020), MICP precipitation kinetics

Yuze Wang, Assistant Professor, PhD, Department of Ocean Science and Engineering, Southern University of Science and Technology, Shenzhen, People's Republic of China (corresponding author). E-mail: wangyz@sustech.edu.cn

(Kim et al. 2020; Wang et al. 2021; Xiao et al. 2021), micro-scale changes with pH variations during MICP treatment (Zehner et al., 2020), and the role of bacteria in MICP and its effects on MICP processes and kinetics (Wang et al. 2021). In addition, microfluidic chip experiments have also been used for studying EICP (Kim et al. 2020, Zehner et al. 2021, Weinhardt et al. 2021). Unlike core scale or model scale soil experiments, microfluidic chip experiments are capable of observing bacterial behaviour and monitoring the whole precipitation processes of calcium carbonate in the porous medium under conditions that mimic the flow conditions in the soil matrix. This provides an opportunity to further explore the microscale mechanisms of MICP or EICP, which will help to advance the understanding the of engineering behaviours of MICP-treated soils."

C2. L140-142. Were the solutions injected from bottom to top?

R1: A sentence was added to explain this experimental procedure more clearly (please see lines 191-193 in the revised manuscript):

"After sand was placed in the columns and saturated with deionized water, injections of bacterial suspension and cementation solution were performed from top to bottom of the soil columns via gravity using the same staged-injection procedure as in the microfluidic chip experiments."

C3. L188-189. Was the amount of chemicals remained in the outlet tube deducted?

R3. A few sentences were added to explain the amount of chemicals being injected and the chemicals considered for calculating the chemical efficiencies as below (please see lines 200-203 in the revised manuscript):

"The tube had an inner diameter of 5 mm, and when the tube was bent upwards, the liquid in the tube was of the same height as the liquid in the soil column. The volume of liquid in the tube was about 5% of the volume of liquid in the soil pores. The amount of chemicals remaining in the outlet tube and above the soil column were not included in the calculation of chemical transform efficiency, since they were not within the soil matrix."

Yuze Wang, Assistant Professor, PhD, Department of Ocean Science and Engineering, Southern University of Science and Technology, Shenzhen, People's Republic of China (corresponding author). E-mail: wangyz@sustech.edu.cn

C4. L207-211. The descriptions are confusing. I am not sure whether the area percentage of dense small crystals or large crystals was 0%.

R4. The description restructured as shown below (please see lines 265-267 in the revised manuscript):

> **"**The 0.6 mm by 0.6 mm squares were valued as 0% when the square was occupied by dispersed large crystals, as shown in Figure 2c, whereas was valued as 1% when the square was mainly occupied by dense small crystals, as shown in Figure 2e. The crystal precipitation pattern of the 6 mm by 6 mm square was quantified"

C5. L288. The term "IN" means injection number?

R5. Yes. "*IN* is the number of cementation solution injections." was added to make it clearer (please see lines 178-179 in the revised manuscript).

C6. L300-301. Which types of crystals remain stable?

R6. "Both large and small crystals" was added before "remain stable" (please see lines 442-443 in the revised manuscript):

C7. L347. Figure 8b did not have purple cycles.

R7. The purple cycle is not clearly shown, therefore yellow arrows are added to communicate the information in a better manner. Please see the revised figure (Figure 8c in the revised manuscript and revised corresponding context in line 348 in the revised manuscript "purple cycled and yellow arrows noted in Figure 8c".

C8. L363-366. Crystal 1, 2, and 3 did not shown in Figure 9.

R8. To avoid confusing, the description below in the submitted version was deleted as the information was not shown in the figure:

"However, the morphology of crystal 1 after the sixth injection and the morphology of crystals 2 and 3 after the second injection of cementation solution is not exactly rhombohedral. A similar phenomenon was observed by Mitchell and Ferris (2006); crystal morphology appeared poorly

Yuze Wang, Assistant Professor, PhD, Department of Ocean Science and Engineering, Southern University of Science and Technology, Shenzhen, People's Republic of China (corresponding author). E-mail: wangyz@sustech.edu.cn

ordered and a stepped surface topography resulted in somewhat rounded crystal edges. New crystals formed between the 6th and 12th injections of cementation solution are rhombohedral."

C9. L399-401. How to confirm that the material marked as Crystal 1 was crystal rather than cells-calcium ions aggregate.

R9. The content related to this description is deleted in the revised manuscript since it is part of the main message and therefore not necessary to be included in this manuscript. This was also deleted to shorten the results of microfluidic chip experiment section.

C10. L405-406. Did the authors mean that Crystal 3, 4, and 5 are kept and growing?

R10. "By 24 hours, the spherical $CaCO_3$ (Crystal 2) crystals dissolve while the more stable three rhombohedral crystals (Crystal 2, 3, 4) become larger." was deleted in the revised manuscript because it is not necessary in deriving the conclusions of this manuscript and to also shorten the results of microfluidic chip experiment.

C11. L471-472. Figure 11 shows microscope images not SEM.

R11. "Figure 11" was corrected to be "Figure 13".

C12. L989. What are the hollow samples in Figure 12(c)?

R12. The Figure 12 (c) was redrawn and enlarged to be clearer (Please see Figure 10 in the revised manuscript).

C13. L1008. The calcium carbonate crystals are supposed to be marked. Which crystal is selected to make a comparison of crystal size?

R13. The calcium carbonate crystals were marked. In addition, three SEM images of Al Qabany & Soga, (2013) was also added for comparison.

Yuze Wang, Assistant Professor, PhD, Department of Ocean Science and Engineering, Southern University of Science and Technology, Shenzhen, People's Republic of China (corresponding author). E-mail: wangyz@sustech.edu.cn

Reply to Reviewer #2:

Reviewer #2's comments are:

"This paper investigates the factors influencing the chemical solution interval of MICP treatment with micro and macro-scale experiments. The topic is partially already reported by the authors. The Micro-scale experiment contains novelty and promotes the bi-soil engineer or researcher. However, the macro-scale experiment is not enough to reach the acceptance level. The authors did not explain the detailed information of microbial species and effective or different characteristics for microbes. (Micro and Macro). In the macro-scale experiments are not enough figures illustrating the results of the experiments. The UCS tests, which quantified the strength behaviors, were not analyzed in detail. Traditional geotechnical testing methods, such as triaxial tests, were not used. Rather than, Compare with published papers of similar topics, this paper did not provide much engineering significance. Overall, the reviewer thinks the manuscript has not met the standard published in a prestigious journal like Acta Geotechnica. The manuscript may better be re-editing of only the micro-scale experiments and submitted to a journal again."

We appreciate Reviewer #2's comments which is very helpful to improve this manuscript. We divided Reviewer #2's comments into six parts and the revisions are as below:

C1. This paper investigates the factors influencing the chemical solution interval of MICP treatment with micro and macro-scale experiments. The topic is partially already reported by the authors. The Micro-scale experiment contains novelty and promotes the bi-soil engineer or researcher. However, the macro-scale experiment is not enough to reach the acceptance level.

R1. The introduction section was revised to clearly state the novelties of this study and to demonstrate the relation of this research with the previous published studies on macroscale experiments including both microfluidic chip experiment and macroscale soil column experiment. This paper fucuses on the link between these two scales of experiments. The macro-scale experiment part was improved and the link between these two experiments was described more clearly. In the introduction section, the previous studies on both microfluidic chip experiment and macroscale soil column experiment were reviewed, the difference of these two types of experiments was described and the objectives and novelties presented in

Yuze Wang, Assistant Professor, PhD, Department of Ocean Science and Engineering, Southern University of Science and Technology, Shenzhen, People's Republic of China (corresponding author). E-mail: wangyz@sustech.edu.cn

this study were described (please see lines 68-116 of the revised manuscript). In the discussion section (the Section 4 in the revised manuscript), the use of microfluidic chips to optimize MICP protocols for strength enhancement was discussed in more details to further illustrate the link between microfluidic chip experiment and soil column experiment.

C2. The authors did not explain the detailed information of microbial species and effective or different characteristics for microbes. (Micro and Macro)

R3. The detailed information of microbial species and effective or different characteristics for microbes (Micro and Macro) were added in the revised manuscript. Please see lines 133-136 in the revised manuscript where the detailed information of microbial species was added as:

> "In the microscale experiment conducted in this study, *Sporosarcina pasteurii* (DSM 33) bacterial suspension was cultivated from a frozen stock purchased from Leibniz Institute DSMZGerman Collection of Microorganisms and Cell Cultures GmbH (Braunschweig, Germany) following the same procedure as described in Wang et al. 2019b until its optical density measured at a wave length of 600 nm (OD_{600}) reached about 1.0. The ureolysis rate of bacteria was determined using the conductivity method described by Whiffin et al. (2007)"

The effective or different characteristics for microbes (Micro and Macro) was added in Lines 193-194 in the revised manuscript as:

> "The bacteria, cultivation procedure, specific activity and retention period were kept the same as described in the microscale microfluidic chip experiment."

C3. In the macro-scale experiments are not enough figures illustrating the results of the experiments.

R3. Two more figures were added to illustrate the results of micro-scale soil column experiments more carefully. These two figures are: "Figure 11. UCS values normalized by $CaCO_3$ content" and "Figure 14. Schematic of $CaCO_3$ crystal precipitation pattern". In addition, In Figure 13, SEM images of $CaCO_3$ crystals inside MICP-treated sand samples after MICP treatments, other three SEM images from previously published paper (Al Qabany & Soga, 2013) was added to compare the crystals characteristic of $CaCO_3$ produced by the nine treatment protocols (Table 2 in the revised manuscript). Further, the

results of micro-scale soil column experiments (Sections 3.4, 3.5 and 3.6 in the revised manuscript) were rewritten to become clearer.

C4. The UCS tests, which quantified the strength behaviors, were not analyzed in detail. Traditional geotechnical testing methods, such as triaxial tests, were not used.

R4. A review of the published research on using USC MICP-treated soils was added (please see lines 81-86 of the revised manuscript) as below:

> "Soil column experiments, which combine carbonate content testing, unconfined compressive strength testing and/or scanning electron microscopy imaging, have been widely conducted as one of the main methods used for studying MICP. The factors and experimental conditions affecting MICP that have been studied include saturation of soil samples (Cheng & Cord-Ruwisch, 2012), bacterial density, reaction time and curing condition (Zhao et al., 2014), particle size distribution (Mahawish et al., 2018), pH (Cui et al. 2020), and concentration of cementation solution (Zhao et al., 2014; Lai et al., 2021)."

The reason to select UCS but not triaxial was added in lines 215-217 of the revised manuscript as below:

> "Since the MICP-treated soil samples are normally rock-like soil specimens, and are stronger than soils, and because UCS test is relatively easier to conduct compared with triaxial testing, it has been widely applied in MICP studies. To compare the results with previously published data, UCS tests were therefore performed in this study."

In Section 3.4, the UCS data were analyzed more carefully, and were compared with previous published research more carefully.

C5. Rather than, Compare with published papers of similar topics, this paper did not provide much engineering significance.

R5. A section "Implications for engineering applications" was added in the revised manuscript (Please see Lines 520-548 in the revised manuscript).

Yuze Wang, Assistant Professor, PhD, Department of Ocean Science and Engineering, Southern University of Science and Technology, Shenzhen, People's Republic of China (corresponding author). E-mail: wangyz@sustech.edu.cn

Use of microfluidic experiments to optimize MICP treatment protocols for effective strength enhancement of MICP-treated sandy soils

Yuze Wang; Charalampos Konstantinou; Kenichi Soga; Jason T. DeJong; Giovanna Biscontin; Alexandre J. Kabla

Author 1

- Yuze Wang, PhD
- Department of Ocean Science and Engineering, Southern University of Science and Technology； Southern Marine Science and Engineering Guangdong Laboratory (Guangzhou) (corresponding author). ORCID: 0000-0003-3085-5299. E-mail: wangyz@sustech.edu.cn

Author 2

- Charalampos Konstantinou
- Department of Civil and Environmental Engineering, University of Cyprus, Nicosia, Cyprus. ORCID: 0000-0002-4662-5327

Author 3

- Kenichi Soga, PhD, FREng, FICE
- Department of Civil and Environmental Engineering, University of California, Berkeley, USA

Author 4

- Jason T. DeJong, PhD
- Department of Civil and Environmental Engineering, University of California, Davis, USA

Author 5

- Giovanna Biscontin, PhD
- Department of Engineering, University of Cambridge, Cambridge, UK

Author 6

- Alexandre J. Kabla, PhD

- Department of Engineering, University of Cambridge, Cambridge, UK. ORCID: 0000-0002-0280-3531

Full contact details of corresponding author.

- Yuze Wang, E-mail: wangyz@sustech.edu.cn; Department of Ocean Science and Engineering, Southern University of Science and Technology, Shenzhen, China

- **Abstract** Microbially-Induced Calcium Carbonate ($CaCO_3$) Precipitation (MICP) has been extensively studied for soil improvement in geotechnical engineering. The quantity and size of calcium carbonate crystals affect the strength of MICP-treated soil. In this study, microfluidic chip experiments and soil column experiments were conducted to optimizate MICP treatment protocols for effective strength enhancement of MICP-treated sandy soils. The microscale experiments reveal that, due to Ostwald ripening, longer injection intervals allow crystals to dissolve and reprecipitate into larger crystals regardless of the concentration of cementation solution. Even though a cementation solution input rate of 0.042 mol/l/h is sufficient to maintain a high chemical transformation efficiency, a further reduction of the input rate by about four times resulted in an increase of the size of crystals produced by the end of treatment from about 40 μm to 60 μm. These findings were applied in soil column experiments. Results showed that significantly larger crystals and higher soil strength were achieved when the normalized rate of cementation solution injection was reduced from 0.042 mol/l/h to 0.021 mol/l/h. Crystal size and soil strength increased slightly more when the normalized input rate was further reduced from 0.021 mol/l/h to 0.010 mol/l/h. This study demonstrates how data from microscale microfluidic experiments that examine the effects of injection intervals and concentration of cementation solution on the properties of calcium carbonate crystals can be used to optimise the MICP treatment in macroscale sand soil column experiments for effective strength enhancement.

Keywords: Microbially-Induced Calcium Carbonate ($CaCO_3$) Precipitation (MICP), microfluidics, microscale properties, strength enhancement, MICP optimization

1. Introduction

Bio-cementation techniques, including Microbially-Inducted Carbonate Precipitation (MICP) and Enzyme-Induced Carbonate Precipitation (EICP), have been introduced in recent years for cementing geological formations such as soils and fractured rocks by using biofluids and chemical solutions to induce carbonate precipitation, thereby cementing geological formations (van Paassen 2009; van Paassen et al. 2010; Dejong et al, 2006, 2010, 2013; Phillips et al. 2013; Lin et al., 2015; Jiang et al., 2017; Chen et al., 2021a,b; Konstainou, 2021a). Due to its ease of control and high chemical transformation efficiency, ureolysis-driven MICP is among the most studied MICP processes (Dhami et al., 2013). During a ureolysis-driven MICP treatment procedure aiming to increase soil strength or to alter soil permeability, ureolytic bacterial suspension (biofluid) is injected into soil, after which a few hours are given for the bacterial cells to settle and attach to soil particle surfaces before cementation solution (which mainly contains urea and $CaCl_2$) is injected into the soil matrix multiple times. The bacteria hydrolyse urea, producing CO_3^{2-}, which reacts with Ca^{2+} to form $CaCO_3$ (equations 1 and 2). The precipitated $CaCO_3$ bonds soil particles, increases the strength of soil matrices and alters soil permeability.

$$CO(NH_2)_2 + 2H_2O \xrightarrow{Urease} 2NH_4^+ + CO_3^{2-} \quad (1)$$

$$Ca^{2+} + CO_3^{2-} \rightarrow CaCO_3(s) \quad (2)$$

Compared to traditional cement, the biofluids which are injected into soil pores or rock fractures have lower viscosities enabling their injection over larger distances, as well as their penetration into smaller fractures (Phillips et al. 2013). In addition, $CaCO_3$ is also more environmentally friendly compared to cement. However, there are still challenges to overcome before MICP can be widely used in real engineering applications. The bio-geo-chemical processes involved in this technique are complex, making it challenging to control and predict the engineering performance of MICP-treated soils at the macro-scale, especially under real environmental conditions. For engineering applications, MICP treatment efficiency needs to be improved significantly in order to become economically viable. Studies have shown that effectiveness of MICP for soil strength enhancement is affected by properties of $CaCO_3$ crystals and the chemical transformation efficiency, the latter of which affects the calcium carbonate content in treated soils (Al Qabany et al., 2012, Al Qabany & Soga, 2013, Cheng et al., 2017).

To overcome the challenges, experimental studies have been conducted to understand the process of MICP and to optimize the treatment protocols. In addition, numerical simulations on MICP have also been developed to link the experiments of MICP to field scale MICP performance. Soil column experiments, which combine carbonate content testing, unconfined compressive strength testing and/or scanning electron microscopy imaging, have been widely conducted as one of the main methods used for studying MICP. The factors and experimental conditions affecting MICP that have been studied include saturation of soil samples (Cheng & Cord-Ruwisch, 2012), bacterial density, reaction time and curing condition (Zhao et al., 2014), particle size distribution (Mahawish et al., 2018), pH (Cui et al. 2020), and concentration of cementation solution (Zhao et al., 2014; Lai et al., 2021).

In recent years, microfluidic chip experiments, have become popular for studying the microscale properties of MICP due to the fact that the *in-situ* behaviour of bacteria and calcium carbonate during MICP treatment can be observed and investigated (Wang et al., 2019a). A microfluidic chip enables the manipulation of small amounts of fluid (Whitesides, 2006) and can replicate key features of the porous matrix of sandy soil such as the shape irregularity of sand grains and pores, as well as the surface properties of the porous channel (Wang et al., 2019a). By performing microfluidic chip experiments, MICP has been further explored in terms of microscale processes (Wang et al.2019b; Kim et al. 2020), MICP precipitation kinetics (Kim et al. 2020; Wang et al. 2021; Xiao et al. 2021), micro-scale changes with pH variations during MICP treatment (Zehner et al., 2020), and the role of bacteria in MICP and its effects on MICP processes and kinetics (Wang et al. 2021). In addition, microfluidic chip experiments have also been used for studying EICP (Kim et al. 2020, Zehner et al. 2021, Weinhardt et al. 2021). Unlike core scale or model scale soil experiments, microfluidic chip experiments are capable of observing bacterial behaviour and monitoring the whole precipitation processes of calcium carbonate in the porous medium under conditions that mimic the flow conditions in the soil matrix. This provides an opportunity to further explore the microscale mechanisms of MICP or EICP, which will help to advance the understanding the of engineering behaviours of MICP-treated soils.

However, the porous media in microfluidic chips are normally two-dimensional structures with the third dimension having the same thickness made using polydimethylsiloxane (PDMS), which do not fully replicate the

three-dimensional features and surface properties of the porous media of soils such as silicon sands. Therefore, the optimized protocols obtained using microfluidic and soil column experimental methods may be different. Since there are not any previous studies that explore the link between these two types of experiments, the primary objective of this study is to compare the similarities and differences between the optimized MICP protocols at the two scales. To link these two experiments, the MICP treatment procedures conducted in these two experiments both use staged-injection procedures, which involve injecting bacterial suspension, after which the bacteria are given several hours to settle and attach to the porous medium prior to applying any subsequent injections of cementation solution. The work presented herein shows the relationship between these two types of experiments and demonstrates how data from microscale microfluidic experiments can be used to enhance the understanding of MICP microscale mechanisms and thereby optimise the MICP treatment of macroscale sand soil samples for effective strength enhancement.

2. Materials and Methods

2.1. Microscale MICP experiments using microfluidic chips

2.2.1 Experimental setup

As described in Wang et al. (2019 a, b; 2021), a microfluidic chip containing porous channels made based on the modified image of a cross-sectional image of real sandy soils is a useful tool to study microscale MICP processes. Figure 1a shows the schematic of the setup for microfluidic chip experiments, which includes a microfluidic chip, a microscope, and a flow injection system consisting of a syringe, a pump and tubing (syringe and pump not shown). The design and fabrication of the microfluidic chip, as well as the detailed imaging technique, are described in Wang et al. (2019a). The microfluidic chip experiment was used to observe the formation of calcium carbonate crystals over time during MICP processes involving multiple injections of cementation solution. Magnified images from previous work (Wang et al., 2019b) are shown in Figure 1a to help identify the microfluidic chip channels, bacteria and crystals.

130

131 *2.2.2 Bacterial medium and cementation solution*

132 In the microscale experiment conducted in this study, *Sporosarcina pasteurii* (DSM 33) bacterial suspension was
133 cultivated from a frozen stock purchased from Leibniz Institute DSMZGerman Collection of Microorganisms and
134 Cell Cultures GmbH (Braunschweig, Germany) following the same procedure as described in Wang et al. 2019b
135 until its optical density measured at a wave length of 600 nm (OD_{600}) reached about 1.0. The ureolysis rate of
136 bacteria was determined using the conductivity method described by Whiffin et al. (2007). The cementation
137 solution contains $CaCl_2$, urea and nutrient broth. The concentrations of $CaCl_2$ and urea varied in different protocols,
138 with either 0.25 M, 0.5 M or 1.0 M $CaCl_2$ together with a 1.5-fold higher concentration of urea being used in each
139 case. In all the protocols, the concentration of nutrient broth is kept constant at 3g/L. The concentration of urea
140 was 1.5 times higher than the concentration of $CaCl_2$ to ensure efficient calcium transformation (Martinez et al.,
141 2013), and the nutrient broth is used to provide nutrients for bacterial cells to maintain their relatively high activity
142 during the injection of cementation solution.
143

144 *2.2.3 MICP treatment procedure*

145 After bacterial suspension, cementation solution and microfluidic chips were prepared, a staged-injection MICP
146 process was applied. In total four protocols were tested (Table 1). In all of the protocols, after the microfluidic
147 chips were saturated with deionized water, 1.25 pore volumes (PVs) of *Sporosarcina pasteurii* (DSM 33)
148 suspension with an OD_{600} of 1.0 and a bacterial activity of 559.0 ± 27.9 mM/h/OD were injected into the
149 microfluidic chips, after which the bacteria were left to attach to the surface of the microfluidic chip channels for
150 approximately 24 hours. Subsequently, multiple injections of 1.25 PVs of cementation solution at different
151 concentrations and injection intervals (retention time) were applied (see Table 1). The injection flow rates of
152 bacterial suspension and cementation solution were 56 PV/h and 5.6 PV/h, which corresponded to Darcy's
153 velocity of 4.6×10^{-4} m/s and 4.6×10^{-5} m/s, respectively. All of the microfluidic chip experiments were

conducted at a room temperature of about 20℃. Protocols M1 and M2 were used to compare the precipitation process when the retention period was 3-5 hours compared to 24 hours, with the concentration of $CaCl_2$ being same in both protocols. In each of these two protocols, 3.0 M × 1.2 pore volumes of $CaCl_2$ were injected. Protocols M3 and M4 were used to compare with Protocol M2 to investigate the difference in the $CaCO_3$ precipitation process when the concentration of cementation solution is varied.

2.1.4 Imaging and image analysis

Imaging of the $CaCO_3$ precipitation procedure in the different protocols was achieved with the use of an Axio Observer Z1 research microscope using phase field illumination and 10× inverted objectives to obtain images with a resolution of 0·65 μm/pixel). Detailed parameters of the microscope are described in Wang et al. (2019a). Images were taken after the end of each retention period after cementation solution injection to analyse the $CaCO_3$ precipitation process in the different protocols.

To quantify the sizes and volumes of crystals in the images, the diameters of each of the crystals in selected areas of the images were measured, and crystal volumes were calculated based on the assumption that the crystals were half spheres (Wang et al., 2019b; Kim et al., 2020). To quantify the number of crystals per unit volume, the numbers of crystals in selected areas of the images were counted, and the number obtained was divided by the corresponding void volume of the microfluidic chip channels (V_v), which was calculated by multiplying the depth of microfluidic chip channels (50 μM) by the area of the selected images. To quantify the total amount of crystals, the total volume of the crystals in selected areas of the images V_c and the corresponding void volume of the channels V_v were obtained first and then V_c /V_v was calculated to determine the normalized crystal volume. Assuming that 100% of Ca^{2+} ions transform into $CaCO_3$, then the V_c /V_v, denoted as $V_{c100\%}$/V_v, can be calculated as:

$$\frac{V_{c100\%}}{V_v} = \frac{[Ca^{2+}] \times IN \times 100 g/mol}{2.71 g/cm^3} \times 100\% \quad (3)$$

where $[Ca^{2+}]$ is the concentration of Ca^{2+} in the cementation solution with mol/L in unit, *IN* is the number of cementation solution injections. Based on the above equation, the chemical transform efficiency (CTE) is calculated using the following formula:

$$CTE = \frac{\frac{V_c}{V_v}}{\frac{V_{c100\%}}{V_v}^3} \times 100\% = \frac{V_c}{V_{c100\%}} \times 100\% \quad (4)$$

2.2. Macroscale MICP experiments

2.2.1. Sand and sample preparation

Macroscale MICP experiments were conducted using the setup same as described in Al Qabany& Soga (2013). The schematic of the experiment is shown in Figure 1b. Syringes with a length of 120 mm and a diameter of 35.4 mm were filled with sand. The granular material was the same as in (Al Qabany et al., 2012, Al Qabany and Soga, 2013), which is poorly-graded sub-rounded sand with a D_{10} value of 165 µm, a D_{90} of 250 µm and specific gravity of 2.65. Each column was filled with 180 g of sand and was vibrated to achieve a final density of 1.65 g/cm^3 and a porosity of about 0.37.

After sand was placed in the columns and saturated with deionized water, injections of bacterial suspension and cementation solution were performed from top to bottom of the soil columns via gravity using the same staged-injection procedure as in the microfluidic chip experiments. The bacteria, cultivation procedure, specific activity and retention period were kept the same as described in the microscale microfluidic chip experiment. In addition, cementation solution content, ratio of urea to $CaCl_2$ and nutrient broth concentration were also the same as in the microfluidic chip experiments. 1.2 PV of bacterial suspension or cementation solution was injected in each injection to ensure all of the soil pores were replaced with a new batch of cementation solution and to ensure the liquid covered continuously the top of the sands specimen during both the injection and retention periods (Al Qabany et al., 2012). During the retention period, the outlet tube was bent upwards to ensure column saturation (Figure 1b). The tube had an inner diameter of 5 mm, and when the tube was bent upwards, the liquid in the tube was of the same height as the liquid in the soil column. The volume of liquid in the tube was about 5% of the

volume of liquid in the soil pores. The amount of chemicals remaining in the outlet tube and above the soil column were not included in the calculation of chemical transform efficiency, since they were not within the soil matrix.

In total, six different MICP treatment protocols (involving different concentrations of cementation solution and retention periods) were applied in the soil column experiments (see Table 2). Table 2 also refers to the protocols of Al Qabany & Soga (2013) for comparison. Triplicate samples were prepared and tested for each protocol. Although the concentration of cementation solution varied (see Table 2), the total mass of cementation solution injected in terms of the available reactants was kept constant across tests by applying more injections at lower concentrations, or fewer injections at higher concentrations, each of which were 3.0 M (indicated by the concentration of $CaCl_2$) × sample liquid volume. All of the sand column experiments were conducted at room temperature of about 22±2℃

2.2.2. Unconfined compression strength (UCS) tests

Since the MICP-treated soil samples are normally rock-like soil specimens, and are stronger than soils, and because UCS test is relatively easier to conduct compared with triaxial testing, it has been widely applied in MICP studies. To compare the results with previously published data, UCS tests were therefore performed in this study. Upon completion of the MICP treatments for the soils in the columns, the specimens were flushed with two pore volumes of deionised water to flush all excess soluble salts prior to removing the specimen from the columns and drying them at 100°C for at least 24 hours before conducing unconfined compression strength (UCS) tests. Since moisture conditions affect the UCS results of tested samples, it is common practice to oven-dry the MICP-treated soil samples (Al Qabany and Soga, 2013; Gomez et al., 2015; Cheng et al.,2017; Mahawish et al., 2018a, Terzis and Laloui, 2018, Terzis and Laloui, 2019, Konstantinou et al. 2021b, Konstantinou 2021c,d). The top and bottom parts of the samples were trimmed to remove potentially disturbed or uneven zones. The UCS experiments were conducted following the ASTM (1986) D2938-86 and ASTM (2004) D7012-14e1 standard test method for intact rock core specimens. The axial load was applied at a constant rate of 1.14 mm/min. The length of the sample was

measured before UCS tests, and the height to diameter ratios were about 2:1, with any deviations being corrected based on Equation 5 as suggested by the ASTM D2938-86-standard test method:

$$C = \frac{C_a}{0.88 + (0.24\,D/H)} \quad (5)$$

where C is the computed compressive strength of an equivalent H/D=2 specimen; C_a is the measured compressive strength; D is the core diameter; and H is its height.

2.2.3. Assessment of $CaCO_3$ content and chemical efficiency

Calcium carbonate ($CaCO_3$) content and chemical efficiency are generally quantified for MICP-treated samples to evaluate the amount of $CaCO_3$ formed in the soil columns, the percentage mass of calcium ions and urea that transformed to $CaCO_3$. Their comparison enables the development of a better understanding of MICP behaviours aiming to eventually optimize MICP treatment protocols. The $CaCO_3$ content of MICP-treated soil samples was determined using the standard test method for rapid determination of carbonate content of soils (ASTM, 2004, D4373-14). About 20 to 30 grams of MICP-treated silicon sand were placed in the reaction chamber and the $CaCO_3$ in the specimen reacted with HCl generating CO_2 (Equation 6) which in turn increased the pressure inside a closed chamber. The actual amount of $CaCO_3$ was calculated based on a calibrated relationship (Equation 7) between the CO_2 pressure and the amount of pure analytical grade $CaCO_3$ powder (ASTM, 2004). $CaCO_3$ content is defined as the calculated mass of $CaCO_3$ divided by the mass of pure sand containing the $CaCO_3$.

$$CaCO_3 + 2HCl \rightarrow CaCl_2 + CO_2 \uparrow + H_2O \quad (6)$$

$$CaCO_3\ mass(g) = pressure \times 1.922 + 0.011 \quad (7)$$

The mass of $CaCO_3$ produced in the soil is affected by the amount of $CaCl_2$ and urea injected into the soils and by the chemical efficiency. Chemical efficiency is defined as the percentage ratio of the measured mass of $CaCO_3$ actually produced, divided by the theoretical mass of $CaCO_3$ which would have been obtained assuming that all the $CaCl_2$ injected into the soil pores is transformed into $CaCO_3$ (Al Qabany et al., 2012; Martinez et al. 2013; Terzis and Laloui. 2016).

252 *2.2.4. Scanning Electron Microscopy (SEM)*

253 To characterise the shapes, sizes and distribution of precipitated $CaCO_3$ crystals inside the soil specimens,
254 scanning electron microscope (SEM) images of MICP-treated soil samples were captured after the UCS test using
255 a Philips XL20 scanning electron microscope (Philips Electron Optics, Eindhoven, The Netherlands). The tested
256 samples were dried in an oven at 100.5°C for 24 hours. Images were taken at 300× magnification.
257

258 # 3. Results

259 ## 3.1. Precipitation process and time-dependent characteristics of crystals in short injection interval
260 case (Protocol M1)

261 To observe the $CaCO_3$ precipitation process in the short injection interval protocol (Protocol M1), images of 6
262 mm by 6 mm square in the middle of the microfluidic chip taken at the completion of the injection intervals
263 between two adjacent cementation solution injections are shown in Figure 2a. To analyse the crystal precipitation
264 patterns, a red grid was placed to divide the image into 100 of 0.6 mm by 0.6 mm cells (small squares), as shown
265 in Figure 2b, d. The 0.6 mm by 0.6 mm squares were valued as 0% when the square was occupied by dispersed
266 large crystals, as shown in Figure 2c, whereas was valued as 1% when the square was mainly occupied by dense
267 small crystals, as shown in Figure 2e. The crystal precipitation pattern of the 6 mm by 6 mm square was quantified
268 by adding the values of the small squares. The quantification result of Figure 2a by this method is shown in Figure
269 2f. It can be seen from both Figures 2a and 2f that, after the first injection of cementation solution, the pore space
270 in the microfluidic chip was mainly precipitated by dispersed large crystals. However, after the second injection
271 of cementation solution, dense small crystals started to precipitate and were stable until the completion of the 12^{th}
272 injection of cementation solution.
273

274 To observe the precipitation behaviour of $CaCO_3$ crystals in Figure 2a in detail, one of the middle sections in the
275 microfluidic chip taken at the completion of each cementation solution injection event is shown in Figure 3. The

crystals formed after the first injection were large and remained present after the final injection (indicated by arrows in the first and 12th images of Figure 3). In addition, some other large crystals formed after the second injection (indicated by cycles in the second and 12th images of Figure 3). The small crystals shown after the 12th injection were mainly formed after the second injection of cementation solution. In general, the crystals continued growing once formed during the 12 injections of cementation solution.

To quantify crystal sizes during the treatment procedure of protocol M1 (short injection interval), images of 2 mm by 2 mm square taken at the centre of the microfluidic chip were selected. Images taken at 3 hours after the completion of the first and the last injection of cementation solution (Figure 4a and b, respectively) show that the crystals were mainly large crystals after the first injection (red cycled noted), whereas after the last injection, there were both large (red and blue cycled noted) and small crystals (white dots). Since the number of large crystals were relatively small therefore all of the crystals could be measured, the diameters of crystals shown in the square (Figure 4 a) after each of the injections of cementation solution were measured. However, the number of small crystals in this area was enormous and it was difficult to measure all of them, therefore 12 of 70 μm by 70 μm squares (noted as blue squared shown in Figure 4c) in the pores at the centre 2 mm by 2mm area of the microfluidic chip were randomly selected, and the magnified image of one calculate zone is shown in Figure 4b. The number of small crystals was counted and the diameters were measured. The total volumes of the crystals relative to the total volume of the calculated zone were calculated. The quantification results of large and small crystals are shown in Figure 5.

The Box plots of the diameters of large crystals at completion of the injection intervals after the 1st, 3rd, 5th, 8th and 12th injections are shown in Figure 5a. The Box plots of the diameters of small crystals at the completion of the injection intervals after the 3rd, 4th, 5th, 7th, 8th and 12th injections are shown in Figure 5b. The mean diameter of the large crystals after the first injection of cementation solution is about 30 μm, and the diameter increases to about 42 μm by the completion of the last injection. The mean diameter of the small crystals after the third injection of cementation solution is about 6.5 μm, and the diameter increases to about 9 μm by the completion of the last injection. The number of the large crystals over the 12th injections of cementation solution remains almost

303 constant and is about 100 per 1 mm^3. The number of the small crystals is about 80 - 400 crystals present per 10^6
304 μm^3, which equals to 8×10^4 - 4×10^5 per 1 mm^3.
305
306 The total volumes of the crystals (V_c) relative to the volumes of the voids (V_v) in the 2 mm by 2 mm calculated
307 zone is plotted with the injection number (Figure 5c). The ratio V_c/V_v for large crystals increases linearly with the
308 increase of injection number, from about 1% after the first injection of the cementation solution to about 2.3%
309 after the last injection. The *Vc*/*Vv* for small crystals increases from about 1.5% after the third injection of the
310 cementation solution to about 4.4% after the 7th injection. Then the growth rate of the small crystals starts reducing
311 and only increases by about 1.6 during the last 5 injections (from the 7th to the 12th injection). The V_c/V_v for all
312 large crystals and small crystals increases from about 1% to about 8% over the 12 injections of cementation
313 solution. In the short injection interval, the large numbers of small crystals contribute to about 2/3 of the whole
314 precipitation (Figure 5c). The growth rate to all the crystals gradually reduces from about 1% per injection between
315 the first to the 3rd injection, to about 0.9% per injection between the 3rd injection to the 5th injection, to about 0.47%
316 per injection between the 5th to the 8th injection, and then to about 0.35% per injection between the 8th to the 12th
317 injection (Figure 5c). This is consistent with the reduction of chemical transformation as the injection number
318 increases (Figure 5d). The chemical transformation efficiency is between 100% during the first to the 5th injection,
319 then reduces to about 85% after the 8th injection, and further reduces to about 69% after the 12th injection (Figure
320 5d). The reduction of chemical transform efficiency the injection numbers increasing might be due to the reduction
321 of bacterial cell number by the injection of cementation (Wang et al., 2019a).
322

323 **3.2. Precipitation process and time-dependent characteristics of crystals in long injection interval case**
324 **(Protocol M2)**

325 To study the effects of prolongation of injection interval on the precipitation process of MICP, protocol M2 with
326 an injection interval of 24 hours was conducted. The precipitation process of the $CaCO_3$ crystals in Protocol M2
327 is shown in the 6 mm by 6 mm images of the same microfluidic chip taken at the completion of the injection
328 interval after each of the cementation solution injections (shown in Figure 6a). The quantification result of Figure

6a by the method described in section 3.1 is shown in Figure 6b. After the first injection of cementation solution, the pore space of the microfluidic chip was mainly precipitated by dispersed large crystals, but after the second injection of cementation solution, dense small crystals started to precipitate. The dense small crystals occupation continued expanding until the 3rd injection to about 100%, after which the area of dense small crystals started reducing to about 20% by the 12th injection of cementation solution.

To observe the precipitation behaviour of $CaCO_3$ crystals in Figure 6a in detail, one of the middle sections in the microfluidic chip taken at the completion of the injection interval of each of the cementation solution injections are shown in Figure 7. The crystals formed after the first injection were large and remained present after the final injection (indicated by arrows in the first and 12th images of Figure 7). In addition, some other large crystals formed after the second injection (indicated by cycles in the second and 12th images of Figure 7). The growth behaviour of the small crystals is different from that in the short injection interval case. The dissolution of both small and large crystals can be seen in this case (Figure 7) which was not shown in the short injection interval case (Figure 3).

To quantify the growth rate of the crystals in protocol M2, same as the short injection interval case, same area from the images is selected (Figure 8a). The large crystals at the completion of the last injection are partially from the ones after the first injection (red cycled noted in Figure 8a and 8b), and partially from the other injections (blue cycled noted noted in Figure 8b). In addition, apart from the fact small crystals dissolve, some of the large crystals that precipitate earlier can also dissolve in the later injections (purple cycled and yellow arrows noted in Figure 8c). This indicates that not only the small crystals can dissolve, some of the large ones can also dissolve in the long injection interval case. The ratio of the dissolved large crystals is about 10%. The Box plots of the diameters of large crystals that appeared from the first injection measured at the completion of the injection intervals after the 1st, 3rd, 5th, 8th and 12th injections are shown in Figure 8d. The mean diameter of the crystals after the first injection of cementation solution is about 30 μm, which is the same as the short injection case (Figure 5a) and the diameter increases to about 60 μm by the completion of the last injection, which is larger than that in the short injection interval case (Figure 5a). The V_c/V_v values of the total volumes of all large crystals increases linearly from about 0.8% to about 9% over the 12 injections of cementation solution (Figure 8e). The chemical

transformation efficiency indicated by only large crystals remains between about 75 to 85% over the 12th injections (Figure 8f). The high chemical transform ratio calculated by only considering large crystals indicating that the majority of crystals in the long injection interval case are large crystals is different to that for the short injection interval, where the small crysatls (crystals size smaller than 10 μm) contribute to about 2/3 of the whole precipitation (Figure 5c). Because the quantification of the small crystals was not conducted in this case, the chemical transformation efficiency would be higher than the reported value, especially in the first few injections when the small crystals were still widely occupied in the channels (Figure 7). Therefore, the total chemical efficiency considering all crystals should be similar to the one in the short injection case (Figure 5d), in which the transform efficiency was higher in the first few injections than that in the later injections.

3.3. Precipitation-disolution of $CaCO_3$ in higher concentrations of cementation solution cases (Protocols M3 and M4)

The concentrations of cementation solution normally used for MICP treatment are between 0.25 M and 1.0 M. To investigate whether the precipitation-dissolution-reprecipitation process also occurs when the concentration of cementation solution was 0.5 M or 1.0 M, protocols M3 and M4 were conducted. A long injection interval of 24 hours was used for each injection. Microscope images of 250 μm × 250 μm at 1, 3, 6 and 24 hours after the completion of the second and first injection of cementation solution for the 0.5 M and 1.0 M case are shown in Figure 9a and 9b, respectively. Similar to what was observed in the 0.25 M case, small crystals also formed after the second injection of cementation solution and subsequently dissolved and replaced by larger crystals.

3.4. Correlations between unconfined compressive strength (UCS) and $CaCO_3$ content in MICP-treated sands

To investigate whether the observations made from microfluidic chip experiments can be used to optimize MICP treatment protocols for soil strength enhancement soil column experiments and UCS tests were conducted. All samples failed with a tensile-like failure in unconfined conditions, similar to the results reported in previous research (van Paassen et al. 2010, Al Qabany et al. 2012 and Cheng et al. 2012). Correlations between the $CaCO_3$

content and UCS were normally derived to study the effect of $CaCO_3$ content on the strength of MICP treated soils (Gomez et al. 2015, Cheng et al. 2017, Mahawish et al. 2018a, Terzis and Laloui 2018, Terzis and Laloui 2019, van Paassen et al. 2010 and Rowshanbakht et al. 2016, Al Qabany and Soga 2013). The correlations between the $CaCO_3$ content and UCS of this study and Al Qabany and Soga (2013) are shown in Figure 10c.

It can be seen from Figure 10 that, UCS varies from 1.8 to 5.6 MPa at the same $CaCO_3$ content of 7%, for example. These large strength variations at the same cementation level are consistent with the results reported by Wang et al. (2017) because the $CaCO_3$ crystals have different characteristics depending on the MICP treatment protocols. In addition, when the concentraions of cementation solution is the same, higher UCS values were obtained when the injection interval was longer. For example, when the concentration is 0.5 M, the 48 hours injection interval (noted as solid round dots) results in UCS values between about 3 Mpa and 5.5 Mpa at $CaCO_3$ content between 6.4% and 7.4%, whereas the 12 hours injection interval (noted as hollow round dots) results in UCS values of only 0.4 Mpa to 1.2 Mpa at similar $CaCO_3$ content range. Further, the UCS values of samples treated with 1.0 M cementation solution are in general lower than the values of samples treated with cementation solution of 0.25 M or 0.5 M when the injection interval is the same. The low UCS values at 1.0 M is mainly because of the inhomogeneity of samples (Al Qabany and Soga, 2013).

To compare the efficiency of $CaCO_3$ in increasing strength of soils, normalized UCS values are obtained by dividing the UCS values with the $CaCO_3$ content of each of the dots in Figure 10 (results shown in Figure 11). The data obtained for the 9 protocols (shown in Table 2) are shown in the 9 columns. For all chemical concentration cases, reducing the normalized input rate resulted to an increase of the efficiency of $CaCO_3$ in terms of enhancing the strength of the specimens (shown when comparing the three columns in each chemical condition case). The normalized UCS values per 1% $CaCO_3$ of samples treated over a 6-day period using 0.25 M, 0.5 M and 1.0 M cementation solution were 3.6.-, 4.9- and 3.9-fold higher than those treated over a period of 3 days, respectively. UCS values increased further by 1.22-, 1.27- and 1.33-, respectively, when the total treatment duration increased from 6 days to 12 days. In addition, the higher the chemical concentration was, the lower the efficiency of $CaCO_3$ in increasing strength of soils was (shown when comparing the three columns of the same

normalized input rate cases). This is consistent with the conclusion obtained by Al Qabany & Soga (2013) that more injections of lower concentrtaions of cementation solution is better for strength enhancing.

3.5 Chemical efficiency of cementation solution transforming into cement in the soil column experiment

The chemical efficiencies quantified in the soil column treated by protocols S2, S3, S5, S6, S8 and S9 (Table 2) are shown in Figure 11. When the concentration of cementation solution was either 0.25 M or 0.5 M, the chemical efficiency was relatively high (higher than 75 %). These results are consistent with the microfluidic chip experiment, as well as the studies conducted by Al Qabany et al. (2012), Cui et al. (2017), and Konstantinou et al., (2021a). In contrast, when the concentration of cementation solution was 1.0 M, the mean chemical efficiency was lower (71% for a 48 h injection interval treatment and 64% for 48 h injection interval treatment), since the long injection intervals likely caused a decrease in bacterial activity due to the higher molarity entombing some of the bacteria over time. However, the bacterial activity inside the soil is difficult to measure. In addition, the variation in chemical efficiency between samples treated with the same MICP procedure, shown by the error bars in Figure 11, was large when the cementation solution concentration was 1.0 M. The large variations in efficiencies indicate the inhomogeneity of soil samples, which is consistent with the results obtained by Al Qabany et al. (2012).

3.6. Microscale properties of $CaCO_3$ crystals obtained by soil column experiment

To observe the $CaCO_3$ crystals after the MICP treatment of the macroscale specimens, scanning electron microscope (SEM) images were taken (see Figure 12). When the concentration of cementation solution is the same, the crystals in the samples treated with longer retention periods are larger than those with shorter retention periods. For example, in the case of 0.25 M concentration, the average size of the crystals increases from about 5 μm at 6 h injection interval, to about 40 μm at a 12-h injection interval, to about 60 μm at 24 h injection interval. The trends of changes in crystals size with the change of injection interval are in agreement with the results obtained in the microscale experiments.

4 Discussion

4.1 Effects of injection interval and concentration of cementation solution on the precipitation processes and characteristics of $CaCO_3$ crystals

Wang et al., 2019b found that precipitation-dissolution and re-precipitation of $CaCO_3$ occurred after a sample of *S. pasteurii* bacterial suspension was mixed with cementation solution, and used this observation to predict and detect the size of calcium carbonate crystals after MICP treatment by using microfluidic chips. To this end, the present study further explores the differences in the precipitation process and time-dependent characteristics of $CaCO_3$ crystals in the cases when long or short injection intervals, as well higer cementation solution concentrations (0.5 M and 1.0 M) were used. When a short injection interval (0.25 M cementation solution with a short injection interval of 3-5 hours) was used, large crystals began to precipitate from the first injection, and small crystals began to precipitate from the second injection (Figures 2 and 3). Both large and small crystals remained stable throughout the whole treatment period (Figures 2 and 3). In the case of a long injection interval (0.25 M cementation solution, 24 hours injection interval), large crystals also precipitated from the first injection onwards and small crystals precipitated from the second injection onwards, but 10% of large crystals and most of the small crystals dissolved (Figures 6 and 7). The dissolution of small or part of the large crystals contributed to the precipitation of larger $CaCO_3$ crystals (Figure 7 compared to Figure 3). When a higher cementation solution concentration together with a long injection interval was used (0.5 M or 1.0 M cementation solution, 24 hours injection interval), more stable crystals grew in size at the expense of the dissolution of less stable crystals during MICP processes (Figures 9). This process of $CaCO_3$ precipitation-dissolution-reprecipitaion when the injection interval is long, regardless of whether the concentration of cementation solution is 0.25 M, 0.5 M or 1.0 M, is consistent with Ostwald ripening, which is a spontaneous process driven by chemical potential differences among different-sized particles; specifically, larger crystals grow at the expense of smaller ones, with the latter having a higher solubility than large crystals (Zhou et al., 2018, Wang et al., 2019a, 2021).

Due to the difference in precipitation process, the average crystal sizes when short or long injection intervals were used were about 40 μm and 60 μm, respectively (Figure 5a and Figure 8d). 8×10^4 - 4×10^5 small crystals per 1

458 mm^3 (sizes smaller than 12 μm by the end of treatment, Figure 5b) in the short injection interval case contributed
459 to about 66% of the whole precipitation (Figure 5c), whereas 100 large crystal crystals per 1 mm^3 of contributed
460 to about 80% chemical transformation efficiency (Figure 8f). The chemical transformation efficiency during the
461 staged-injection MICP treatment procedure reduced as the number of cementation solution injections increased
462 (Figure 5d), possibly because bacterial activity reduced due to the removal of bacterial cells from the porous
463 medium by the injections of cementation solution. In addition, increasing the injection interval from 3-5 hours to
464 24 hours, resulted in an increase of the chemical transformation efficiency from 70% to more than 80% by the
465 end of MICP treatment (Figure 5d compared to Figure 8f). In the staged injection procedure, the biochemical
466 reactions started after the injection of cementation solution into the soil matrix. If the next batch of cementation
467 solution is injected before the previous batch of cementation solution finished transforming into $CaCO_3$, the
468 chemical transformation efficiency of MICP will be low. Al Qabany et al. (2012) conducted a series of soil column
469 experiments to determine the optimal injection interval by varying the injection interval and measuring the $CaCO_3$
470 content at the end of MICP treatment to compare the associated chemical transformation efficiencies. In their
471 study, when the bacterial optical density (OD_{600}) was between 0.8 and 1.2, the chemical efficiency remained
472 higher than 80% provided that the cementation solution injection rate was below a threshold of 0.042 mole/l per
473 hour. By contrast, the chemical efficiency decreased when the injection rate exceeded this threshold. 0.042 mole/l
474 per hour is quivalent to 6 hours retention time for the case when the concentration of cementation solution was
475 0.25 M. The chemical efficicency results observed in the current study are consistent with the results presented in
476 Al Qabany et al. (2012).

477 **4.2 Use of microfluidic chips to optimize MICP protocols for strength enhancement**

478 Studies have found that both $CaCO_3$ content as well as the properties of $CaCO_3$ crystals affect the strength of
479 MICP-treated soils. Soil column experiments, together with UCS testing,triaxial tesing and SEM imaging, are the
480 main methods that have been used so far to optimize treatment protocols for enhancing the strength of MICP-
481 treated soils. However, although MICP optimization using soil column experiments and SEM imaging is
482 important, it is also time-consuming. In contrast to soil column experiments, microfluidic chip experiments
483 provide a functional way to observe the MICP precipitation process directly during each of the injections of

cementation solution (Wang et al., 2019). The time needed for cementation solution to complete transforming into $CaCO_3$ cystals can be directly determined by the finding the time point when the crystals stop growing (Wang et al., 2021). In addition, changes in $CaCO_3$ morphology, and the interactions between bacteria and $CaCO_3$ can also be studied.

In this study, by applying the observations made during microfluidic chip experiments, soils treated using long injection intervals (lower normalized rate of injection) had higher UCS values in samples with similar rage of $CaCO_3$ content (Figure 10). In addition, the normalized UCS values of $CaCO_3$ content were higher when the injection intervals were longer, regardless of the concentration of cemenation solution (Figure 11). The higher normalized UCS values obtained after longer injection intervals indicates that a longer injection interval produced $CaCO_3$ crystals that are more efficient in enhancing soil strength. SEM imaging revealed that crystal sizes were larger when the injection interval was longer compared to crystal sizes that were produced when a short injection interval was used (Figure 12).

Studies have found that crystals which are large enough to fill the gaps between soil particles can prevent particle rotations during shearing, thereby providing more resistance to dilation, which results in increased soil strength (Zhou et al., 2018). This can explain the reason why a longer injection interval is helpful for strength enhancement (Figure 12). In addition, this study has also shown that when the crystals are small and large in number, the crystals precipitate over a large area of the soil surface and form a so-called coating precipitation pattern (Figure 12 a and d). By contrast, when the crystals are large in size and small in number, the crystals either grow on the parts of the surface where they are adjacent to other soil particles, or on parts of the soil surface that face torwards the soil pores, thereby forming a bonding pattern or filling pattern, respectively. The crystals can also form a mixture of two or three of these patterns. For example, during the 2^{nd} to the 8^{th} injections in Figure 7, crystals formed coating, pore filling and bonding patterns, whilst in Figure 12 g and h, crystals formed a mixture of coating and pore filling patterns.

In microfluidic chips, $CaCO_3$ crystals grow from the top and bottom surfaces of the channels, as well as from the sides of pillars (see Figures 3, 7 and 9), whereas in three-dimentional soil matrices, crystals grow on the surfaces

of soil particles. Despite the differences in pore structures between microfluidic chips and real sandy soil matrices, the changes in crystal size and the general crystal distribution (coating, filling and bonding, schemetic shown in Figure 14) shown in the microfluidic chip experiments are the same as shown in the soil column experiment. Therefore, the microfluidic chip experiment can help to predict the $CaCO_3$ crystals distribution pattern. These results indicate that the observation made from microfluidic chip experiments helps to enhance the understanding of microscale processes, mechanisms and characteristics of MICP, which can be applied in real sandy soil for MICP strength enhancement.

5 Implications for engineering applications

This study illustrates that increasing injection interval (reducing normalized input rate of cementation solution) increase the average size of $CaCO_3$, which are more efficient in bonding soil particles and thereby enhancing soil strength. In addition, this research also shows that more injections of lower concentration of cementation solution tend to enhance soil strength more effectively. However, for practicle reasons, the treatment duration and injection numbers of MICP may preferably be minimised. A blance between optimum soil strength enhancement and the time window of MICP-treatment should be considered for MICP engineering applications. The mechanisms of forming higher percentage of $CaCO_3$ crystals which bond soil particles within a short treatment of time and simpler treatment procedure may also be worth exploring in the future.

In order for MICP to be used for real engineering projects, the effects of local environmental factors such as soil properties, ion content, temperature, oxygen content and local bacterial communities on the bahaviour of bacteria, $CaCO_3$ precipitation processes and kinetics, as well as $CaCO_3$ content and microscale characteristics which affect the engineering performance of MICP-treated soils, need to be evaluated beforehand. These effects can be evaluated by performing the microfluidic chip experiments, and understanding these effects will be helpful for improving MICP treatment protocols. Combining microfluidic chip experiments with soil column experiments is a useful way to optimize MICP treatment protocols, especially in terms of enhancing soil strength.

Achieving uniformity of $CaCO_3$ content distribution in soil matrices remains challenging for engineering applications. $CaCO_3$ distribution is highly dependent on the reactive-transport processes of MICP. So far, several numerical models have been proposed for predicting $CaCO_3$ content, but mostly only for lab-scale soil matrices without considering the complex effects of environmental factors on MICP. Inhomogenous samples have been observed even for core scale homogeneously-produced sandy sampleswhen the concentration of cementation solution was 1.0 M. For engineering applications, environmental factors and soil inhomogeneity may affect bacterial and chemical transport, bacterial activity and cementation kinetics, thereby making the distribution of $CaCO_3$ crystals more difficult to predict. Combining microfluidic chip experiments with longer column experiments or 3-D soil model experiments to inverstigate the effects of various environmental factors and treatment protocols on the homogeneity of MICP-treated soils may provide a useful way to address this challenge, which still needs to be further explored in the future.

6 Conclusions

This study demonstrates an example of using a combination of microfluidic chip experiments and soil column experiments for optimizing soil strength enhancement protocols. The effects of injection interval and concentration of cementation solution on the properties of calcium carbonate crystals were examined at both the micro- and the macroscale.

Both the microscale microfluidic chip experiments and macroscale column tests indicated that, when the injection interval was shorter (i.e. 3-5 hours compared to 24 hours for a 0.25 M cementation solution), the resulting crystals were larger in number and smaller in size. In addition, the microscale microfluidic chip experiments showed that large crystals grew at the expense of the dissolution of smaller crystals, regardless of whether the concentration of cementation solution was 0.25 M, 0.5 M or 1.0 M. This could be attributed to Ostwald ripening, a spontaneous process driven by chemical potential differences between different-sized particles, where larger crystals grow at the expense of smaller ones which have a higher solubility than the large ones.

The difference in crystal sizes and numbers substantially affected the strength of MICP-treated specimens. Regardless of concentration of cementation, reducing the normalized input rate of cementation solution from 0.042 mol/l/h (treated over 3 days) to 0.021 mol/l/h (treated over 6 days) significantly increases UCS values of samples, whereas a further reduction of the normalized input rate of cementation solution from 0.021 mol/l/h (treated over 6 days) to 0.010 mol/l/h (treated over 12 days) slightly increases UCS values of samples. The normalized UCS values per 1% $CaCO_3$ using 0.25 M, 0.5 M and 1.0 M cementation solution were 4.3-, 5.8- and 3.2-fold higher than those treated over a period of 3 days, respectively. The normalized UCS values per 1% $CaCO_3$ of samples treated over a 6-day period using 0.25 M, 0.5 M and 1.0 M cementation solution were 3.6.-, 4.9- and 3.9-fold higher than those treated over a period of 3 days, respectively. UCS values increased by a further 1.22-, 1.27- and 1.33-, respectively, when the total treatment duration increased from 6 days to 12 days. The less pronounced increase in the strength of soils treated over 12 days compared to 6 days was largely because over 6 day-treatment, the crystals were already relatively large enough to bond the soil particles efficiently and further crystal growth increased soil strength but to a less extent.

This study shows that increasing injection interval and introducing more injections of lower concentration of cementation solution tend to enhance soil strength more effectively. However, for practicle reasons, the treatment duration and injection numbers of MICP may preferably be minimised. The mechanisms of forming higher percentage of $CaCO_3$ crystals which bond soil particles within a short treatment of time and simpler treatment procedure may also be worth exploring in the future.

The microfluidic chip experiments presented in this research illustrate changes in crystal sizes and numbers with time and provide direct information about the MICP process. This study establishes a link between the results of MICP microscale microfluidic chip experiments and the macroscale column experiments, thereby demonstrating that monitoring microscopic process in microfluidic chip experiments can be useful for optimising MICP treatment to produce calcium carbonate crystals with desired properties for field applications.

Acknowledgements

Y.W. would like to acknowledge the support of National Nature Science Foundation of China, Shenzhen Science and Technology Innovation Commission, Cambridge Trust, and China Scholarship Council. J.T.D. acknowledges the support of the Engineering Research Center Program of the National Science Foundation under NSF Cooperative Agreement No. EEC-1449501. Any opinions, findings and conclusions or recommendations expressed in this manuscript are those of the authors and do not necessarily reflect the views of the National Science Foundation.

References

Al Qabany A and Soga K (2013) Effect of chemical treatment used in MICP on engineering properties of cemented soils. Géotechnique **63(4)**: 331–339.

Al Qabany A, Soga K and Santamarina C (2012) Factors Affecting Efficiency of Microbially Induced Calcite Precipitation. Journal of Geotechnical and Geoenvironmental Engineering **138(8)**: 992–1001.

ASTM (1986) D2938:390-391： Standard test method of unconfined compressive strength of intact rock core specimens. In: 1995 Annual Book of ASTM standards. ASTM, West Conshohocken, PA, USA.

ASTM (2004) D7012-14e1： Compressive Strength and Elastic Moduli of Intact Rock Core Specimens under Varying States of Stress and Temperatures. ASTM, West Conshohocken, PA, USA.

ASTM (2014) D4373-14: Standard Test Method for Rapid Determination of Carbonate Content of Soils. ASTM, West Conshohocken, PA, USA.

Cheng L and Cord-Ruwisch R (2012) In situ soil cementation with ureolytic bacteria by surface percolation. Ecological Engineering **42**: 64–72.

Cheng L, Shahin M A and Mujah D (2017) Influence of Key Environmental Conditions on Microbially Induced Cementation for Soil Stabilization. Journal of Geotechnical and Geoenvironmental Engineering **143(1)**: 04016083.

Chen, Y., Gao, Y., Ng, C. W. W., & Guo, H. (2021). Bio-improved hydraulic properties of sand treated by soybean urease induced carbonate precipitation and its application Part 1: Water retention ability. Transportation Geotechnics, 27(September 2020), 100489. https://doi.org/10.1016/j.trgeo.2020.100489

Chen, Y., Gao, Y., & Guo, H. (2021). Bio-improved hydraulic properties of sand treated by soybean urease induced carbonate precipitation and its application Part 2: Sand-geotextile capillary barrier effect. Transportation Geotechnics, 27(September 2020), 100484. https://doi.org/10.1016/j.trgeo.2020.100484

Cui, Ming-Juan, Zheng, Jun-Jie, Zhang, Rong-Jun, Lai, Han-Jiang, Zhang, Jun. 2017. Influence of cementation level on the strength behaviour of bio-cemented sand. Acta Geotechnica, **12(5)**: 971-986.

DeJong JT, Fritzges MB and Nüsslein K (2006) Microbially Induced Cementation to Control Sand Response to Undrained Shear. Journal of Geotechnical and Geoenvironmental Engineering **132(11)**: 1381–1392

DeJong JT, Mortensen BM, Martinez BC and Nelson DC (2010) Bio-mediated soil improvement. Ecological Engineering **36(2)**:197–210.

DeJong J T , Soga K, Kavazanjian E, Burns S, Van Paassen L A, Al Qabany A, Aydilek A, Bang S S , Burbank M , Caslake L F , Chen C Y, Cheng X, Chu J, Ciurli S, Esnault-Filet A, Fauriel S, Hamdan N, Hata T, Inagaki Y, Jefferis S, Kuo M, Laloui L, Larrahondo J, Manning D A C , Martinez B, Montoya B M, Nelson D C, Palomino A, Renforth P, Santamarina J C, Seagren E A , Tanyu B, Tsesarsky M and Weaver T (2013). Biogeochemical processes and geotechnical applications: progress, opportunities and challenges. Géotechnique **63(4)**: 287–301.

Dhami NK, Reddy MS and Mukherjee A (2013) Biomineralization of calcium carbonates and their engineered applications: a review. Frontiers in Microbiology, **4(October)**: 314.

Gomez, Michael G., Martinez, Brian C., DeJong, Jason T., Hunt, Chris E., deVlaming, Len A., Major, David W., Dworatzek, Sandra M (2015). Field-scale bio-cementation tests to improve sands. Ground Improvement, 168(3), 206–216.

Jiang NJ, Soga K and Kuo M (2017) Microbially Induced Carbonate Precipitation for Seepage-Induced Internal Erosion Control in Sand–Clay Mixtures. Journal of Geotechnical and Geoenvironmental Engineering **143(3)**: 04016100.

Konstantinou C, Biscontin G, Jiang NJ and Soga K (2021a) Application of microbially induced carbonate precipitation (MICP) to form bio-cemented artificial sandstone. Journal of rock mechanics and geotechnical engineering. https://doi.org/10.1016/j.jrmge.2021.01.010

Konstantinou, C, Wang, Y, Biscontin, G, Soga K (2021b) The role of bacterial urease activity on the uniformity of carbonate precipitation profiles of bio-treated coarse sand specimens. Scientific Reports 11, 6161. https://doi.org/10.1038/s41598-021-85712-6

Kim D H, Mahabadi N, Jang J and van Paassen L A (2020). Assessing the kinetics and pore‐scale characteristics of biological calcium carbonate precipitation in porous media using a microfluidic chip experiment. Water Resources Research, 56, e2019WR025420.

Lin H, Suleiman MT, Brown DG, Kavazanjian Jr, E. 2015. Mechanical behavior of sands treated by microbially induced carbonate precipitation. Journal of Geotechnical and Geoenvironmental Engineering, 142:04015066.

Lai, H. J., Cui, M. J., Wu, S. F., Yang, Y., & Chu, J. (2021). Retarding effect of concentration of cementation solution on biocementation of soil. *Acta Geotechnica*, ***16*(5),** 1457–1472. https://doi.org/10.1007/s11440-021-01149-1

Martinez BC, DeJong JT, Ginn TR, Montoya BM, Barkouki TH, Hunt C, Tanyu B, Major D (2013) Experimental Optimization of Microbial-Induced Carbonate Precipitation for Soil Improvement. Journal of Geotechnical and Geoenvironmental Engineering **139**:587–598.

Mahawish, Aamir, Bouazza, Abdelmalek, Gates, Will P. 2018. Improvement of Coarse Sand Engineering Properties by Microbially Induced Calcite Precipitation. Geomicrobiology Journal, 35(10): 887-897.

Phillips, A. J., Lauchnor, E., Eldring, J., Esposito, R., Mitchell, A. C., Gerlach, R., & Spangler, L. H. (2013). Potential CO_2 leakage reduction through biofilm-induced calcium carbonate precipitation. Environmental Science & Technology, 47(1), 142–149.

Xiao, Y., He, X., Wu, W., Stuedlein, A. W., Evans, T. M., Chu, J., Liu, H., van Paassen, L. A., & Wu, H. (2021). Kinetic biomineralization through microfluidic chip tests. *Acta Geotechnica*, *16*(10), 3229–3237. https://doi.org/10.1007/s11440-021-01205-w

Terzis, D., Bernier-Latmani, R., Laloui, L. 2016. Fabric characteristics and mechanical response of bio-improved sand to various treatment conditions. Géotechnique letters, 69(1): 50-57.

Terzis, Dimitrios and Laloui, Lyesse. 2018. 3-D micro-architecture and mechanical response of soil cemented via microbial-induced calcite precipitation. Scientific Reports, 8(1): 1416.

Terzis, Dimitrios and Laloui, Lyesse. 2019. A decade of progress and turning points in the understanding of bio-improved soils: A review. Geomechanics for Energy and the Environment, 19: 100116.

van Paassen L, Ghose R, van der Linden TJM, van der StarWRL and van Loosdrecht MCM (2010) Quantifying Biomediated Ground Improvement by Ureolysis: Large-Scale Biogrout Experiment. Journal of Geotechnical and Geoenvironmental Engineering **136(12)**: 1721–1728.

van Paassen L (2009) Biogrout: Ground Improvement by Microbially Induced Carbonate Precipitation. PhD Thesis, Delft University of Technology.

Wang Y, Soga K and Jiang NJ (2017) Microbial induced carbonate precipitation (MICP): the case for microscale perspective. Proceedings of the 19th International Conference on Soil Mechanics and Geotechnical Engineering, 1099-1102.

Wang Y, Soga K, DeJong JT and Kabla A (2019a) A microfluidic chip and its use in characterizing the particle-scale behaviour of Microbial-Induced Carbonate Precipitation (MICP). Géotechnique **69(12)**:1086-1094

Wang Y, Soga K, DeJong JT and Kabla A (2019b) Microscale visualization of Microbial-Induced Carbonate Precipitation (MICP) processes. Journal of Geotechnical and Geoenvironmental Engineering **145(9)**: 04019045

Wang Y, Soga K, DeJong JT and Kabla A. (2021) Forthcoming. Effects of bacterial density on growth rate and characteristics of microbial-induced $CaCO_3$ precipitates: a particle-scale experimental study. ASCE Journal of Geotechnical and GeoenvironmentalEngineering.https://doi.org/10.1016/(ASCE)GT.1943-5606.0002509

Weinhardt, F., Class, H., Vahid Dastjerdi, S., Karadimitriou, N., Lee, D., & Steeb, H. (2021). Experimental Methods and Imaging for Enzymatically Induced Calcite Precipitation in a Microfluidic Cell. *Water Resources Research*, *57*(3), 1–11. https://doi.org/10.1029/2020WR029361

Whitesides, G. M. (2006). The origins and the future of microfluidics. Nature, 442(7101), 368–373.

Zhou H, Xu S and Sun Z (2018) Real-time in situ observation of shear modulus evolution during Ostwald ripening of colloidal crystallization. Journal of Crystal Growth **502(June)**: 35–40.

Zhao, Q., Li, L., Li, C., Li, M., Amini, F., & Zhang, H. (2014). Factors Affecting Improvement of Engineering Properties of MICP-Treated Soil Catalyzed by Bacteria and Urease. *Journal of Materials in Civil Engineering*, *26*(12), 04014094. https://doi.org/10.1061/(asce)mt.1943-5533.0001013

Zehner, J., Røyne, A., & Sikorski, P. (2021). A sample cell for the study of enzyme-induced carbonate precipitation at the grain-scale and its implications for biocementation. *Scientific Reports*, *11*(1), 1–10. https://doi.org/10.1038/s41598-021-92235-7

Zehner, J., Røyne, A., Wentzel, A., & Sikorski, P. (2020). Microbial-induced calcium carbonate precipitation: an experimental toolbox forin situand real time investigation of micro-scale pH evolution. *RSC Advances*, *10*(35), 20485–20493. https://doi.org/10.1039/d0ra03897k

724

725

726 **Table 1** Parameters of microfluidic chip experiments

Protocol No.	Chemical concentration	Retention time (h)	Normalized input rate (mole/l per h)
M1	0.25 M Calcium chloride	3-5	0.042
M2	0.25 M Calcium chloride	24	0.010
M3	0.5 M Calcium chloride	24	0.021
M4	1.0 M Calcium chloride	24	0.042

727

728 **Table 2** Parameters of macroscale soil column experiments

Protocol No.	Chemical concentration	Retention time (h)	Normalized input rate (mole/l per h)	References
S1	0.25 M calcium chloride	6	0.042	(Al Qabany & Soga, 2013)
S2		12	0.021	This study
S3		24	0.010	This study
S4	0.50 M calcium chloride	12	0.042	(Al Qabany & Soga, 2013)
S5		24	0.021	This study
S6		48	0.010	This study
S7	1.00 M calcium chloride	24	0.042	(Al Qabany & Soga, 2013)
S8		48	0.021	This study
S9		96	0.010	This study

729

730

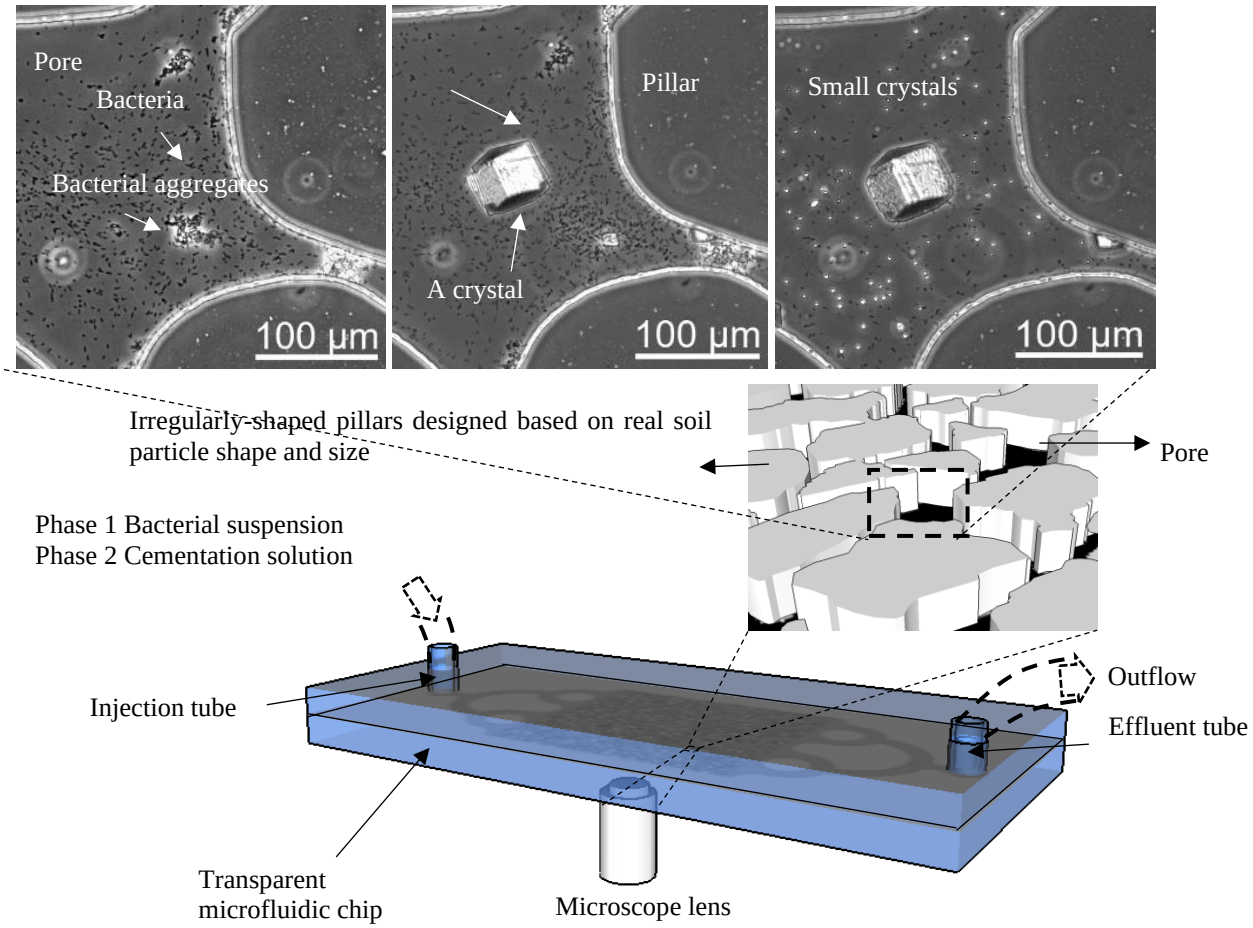
Pore
Bacteria
Bacterial aggregates
100 μm
Pillar
A crystal
100 μm
Small crystals
100 μm
Irregularly-shaped pillars designed based on real soil particle shape and size
Pore
Phase 1 Bacterial suspension
Phase 2 Cementation solution
Injection tube
Outflow
Effluent tube
Transparent microfluidic chip
Microscope lens

(a)

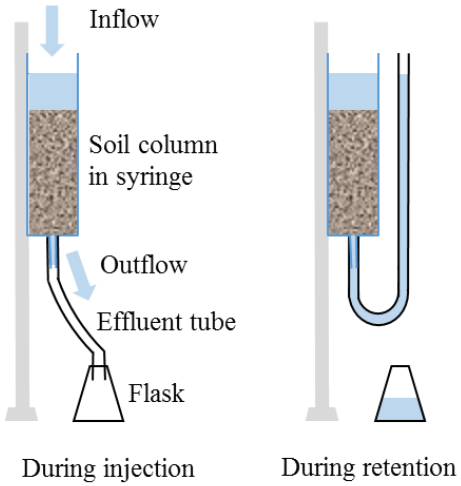
Inflow
Soil column in syringe
Outflow
Effluent tube
Flask
During injection
During retention

(b)

Figure 1 Schematic of experimental setup. (a) microscale microfluidic chip experiments (Wang et al., 2019a); (b) macroscale soil column experiments (redraw based on Al Qabany et al., 2012)

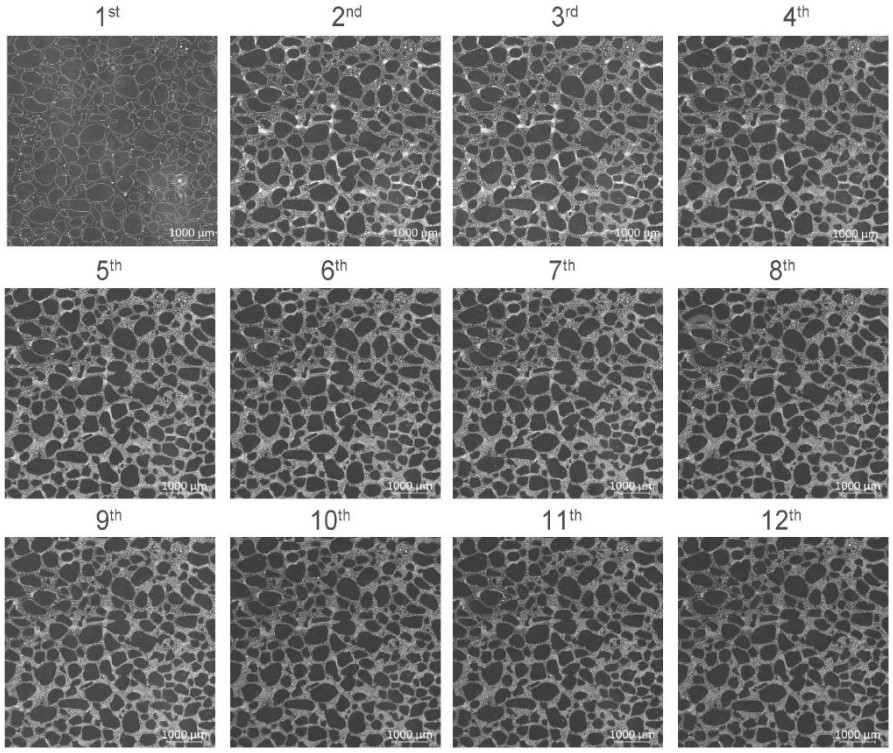

(a)

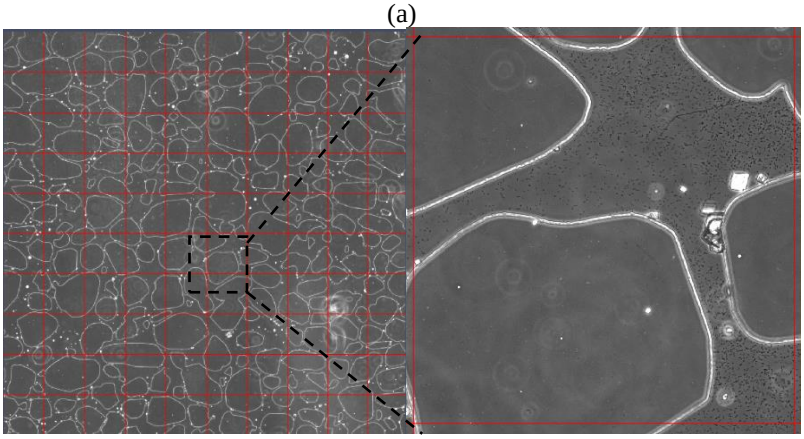

(b) (c)

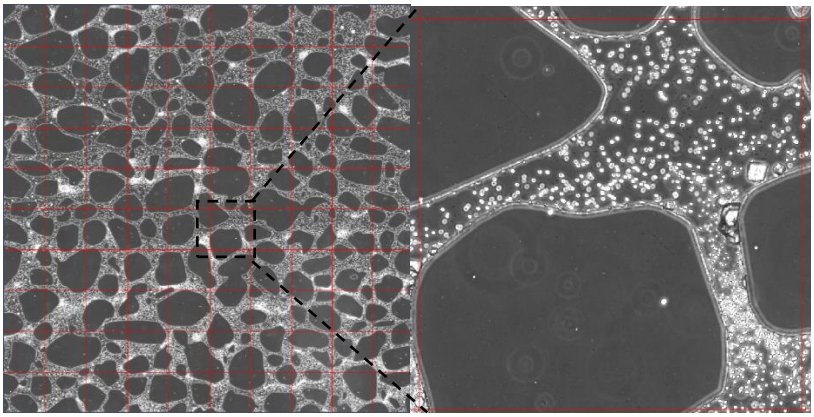

(d) (e)

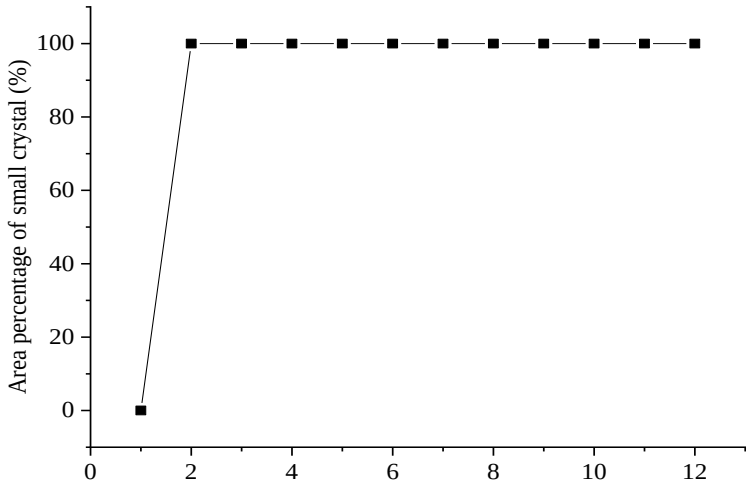

(f)

Figure 2 Crystal growth patten in the short injection interval case. (a) microscope images of the centre 6 mm by 6 mm squares taken at the completion of the injection inteveral of each cementation solution injection; a grid was placed with a cell size of 0.6 by 0.6 mm (b and d), to analyse the precipitation patterns (c and e). (c) crystals were mainly small dense crystals, and the square is counted as 1%; (d) crystals were large dispersed crystals, and the square is counted as 0%; (f) area percentage of small crystals plotted against injection numbers.

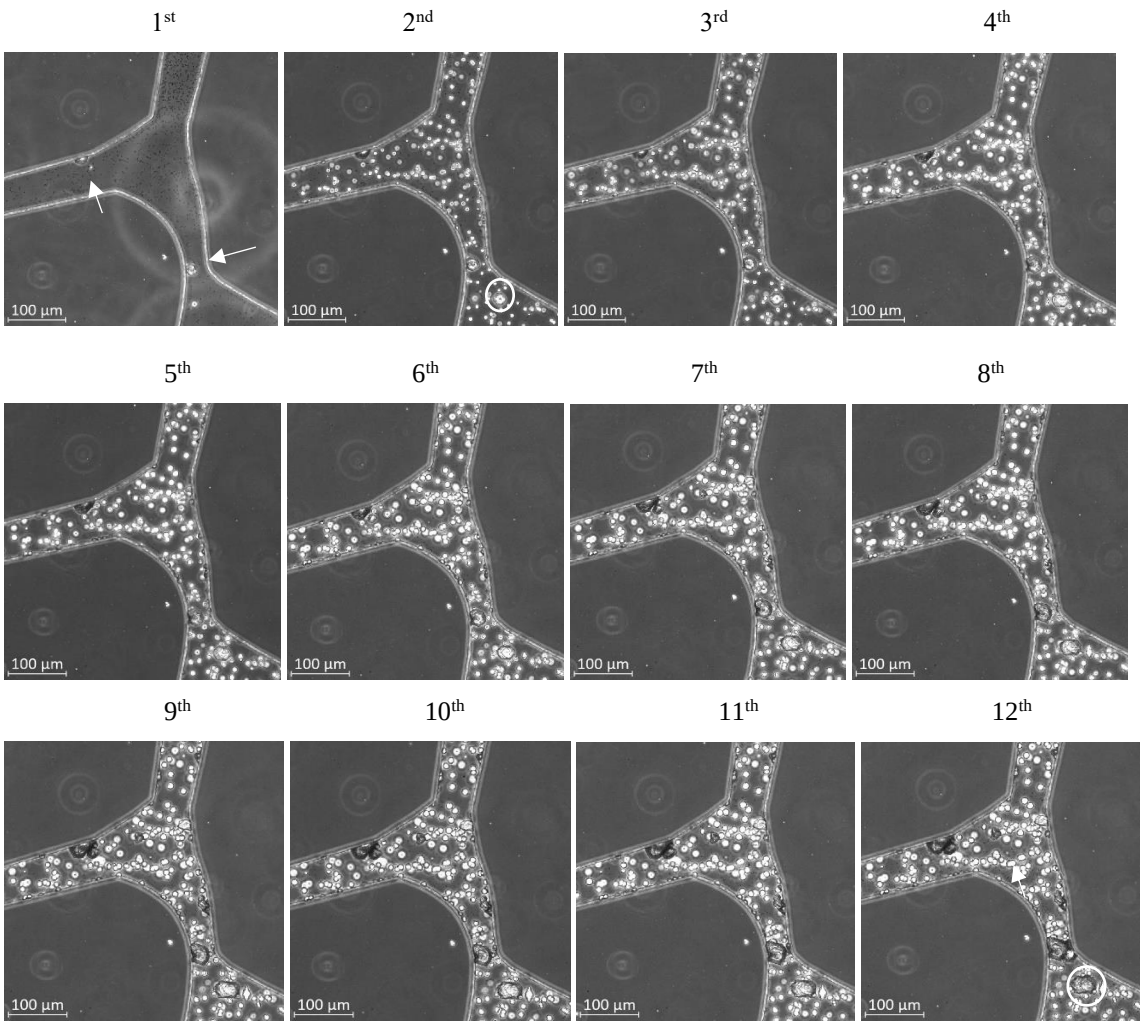

Figure 3 Images taken at the centre of the 6 by 6 mm square after the completion of the injection inteveral of each cementation solution injection (short injection interval case)

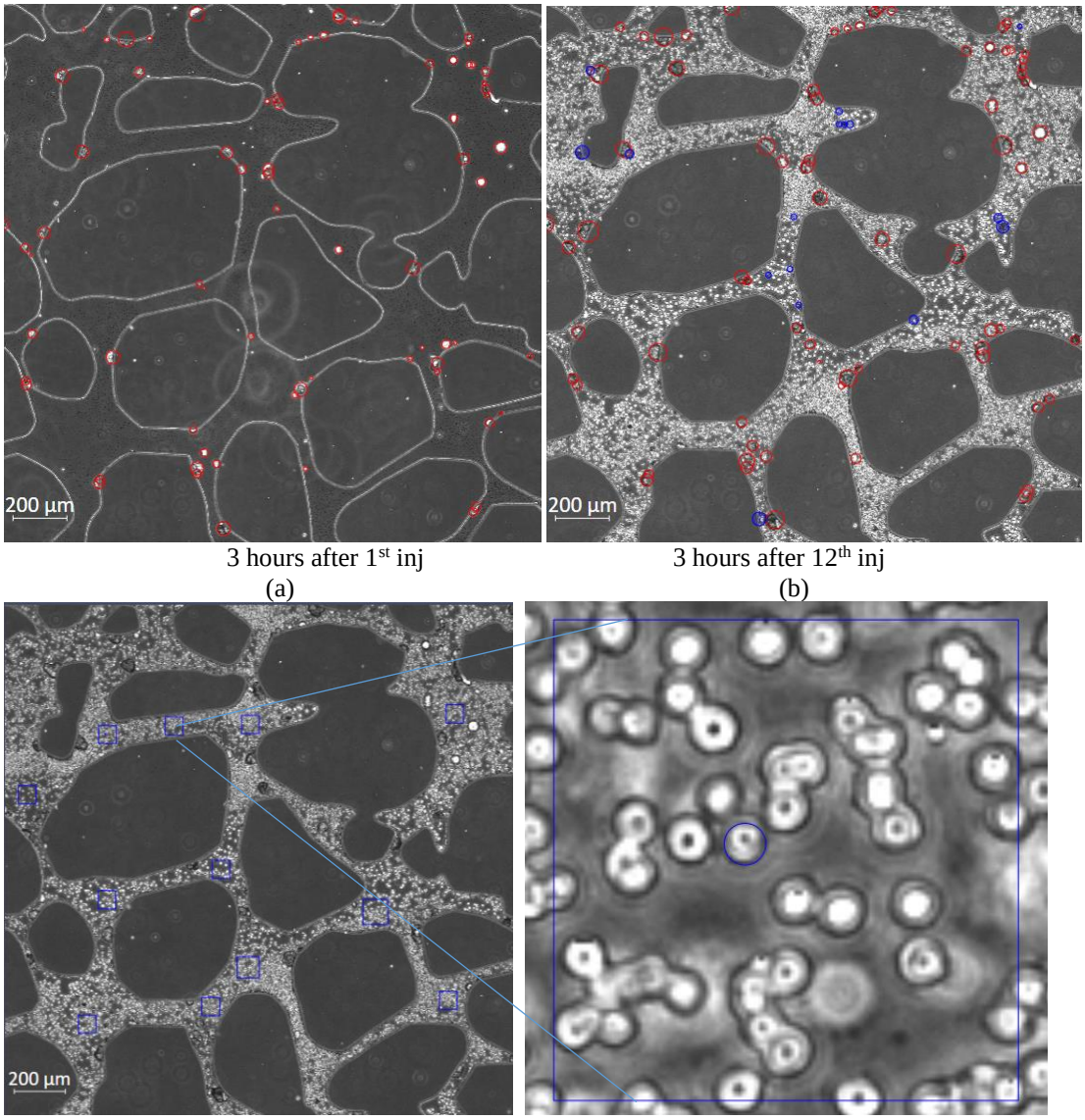

3 hours after 1st inj (a) 3 hours after 12th inj (b)

(c) (d)

Figure 4. Microscope images for quantification. (a-b) Images taken at the centre of the microfluidic chip at the completion of injection interval after the first and the last injections of cementation solution; (c) image taken at the centre of the microfluidic chip at the completion of injection interval after the last injection of cementation solution, with 12 of 70 µm by 70 µm squares for quantifying small crystal size; (d) magnified image of one of the 70 µm by 70 µm squares shown in Figure 4c.

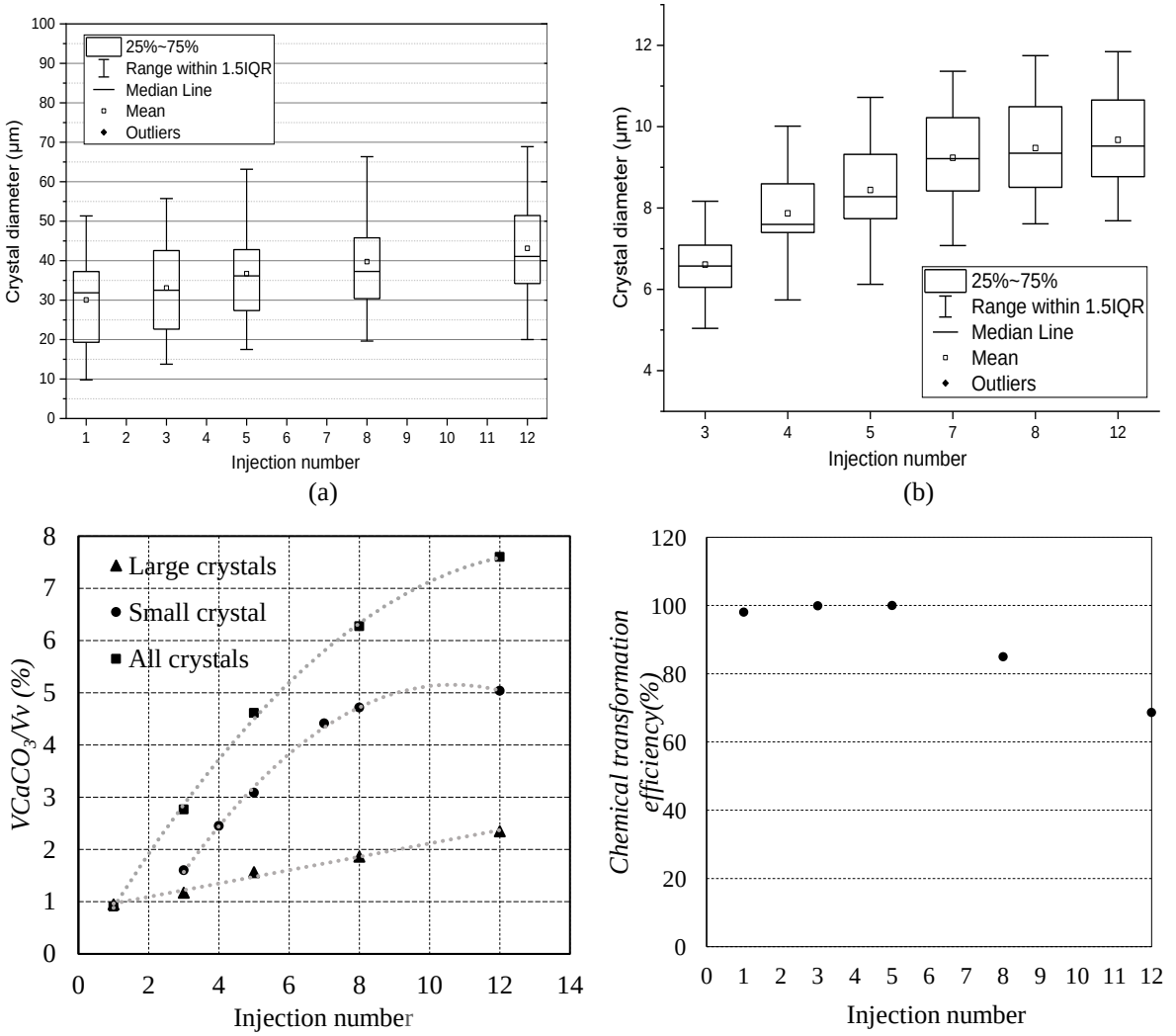

Figure 5 Quantification of crystals formed in protocol M1. (a) Box chart of the diameters of large crystals at completion of the injection intervals after the 1st, 3rd, 5th, 8th and 12th injections; box chart of 12 crystals, each from the 12 squares in Figure 4d, at the completion of injection interval after the 3rd, 4th, 5th, 7th, 8th and 12th cementation solution injection; (c) voild ratio of large, small and all crystals (*Vc*) to the corresponding volume of the voids (V_v) in the 2 mm by 2 mm calculated zone plotted with the injection number; (d) chemical transformation efficiencies of all small and large crystals at the completion of injection interval after the 1st, 3rd, 5th, 8th and 12th cementation solution injection of the short injection interval protocol

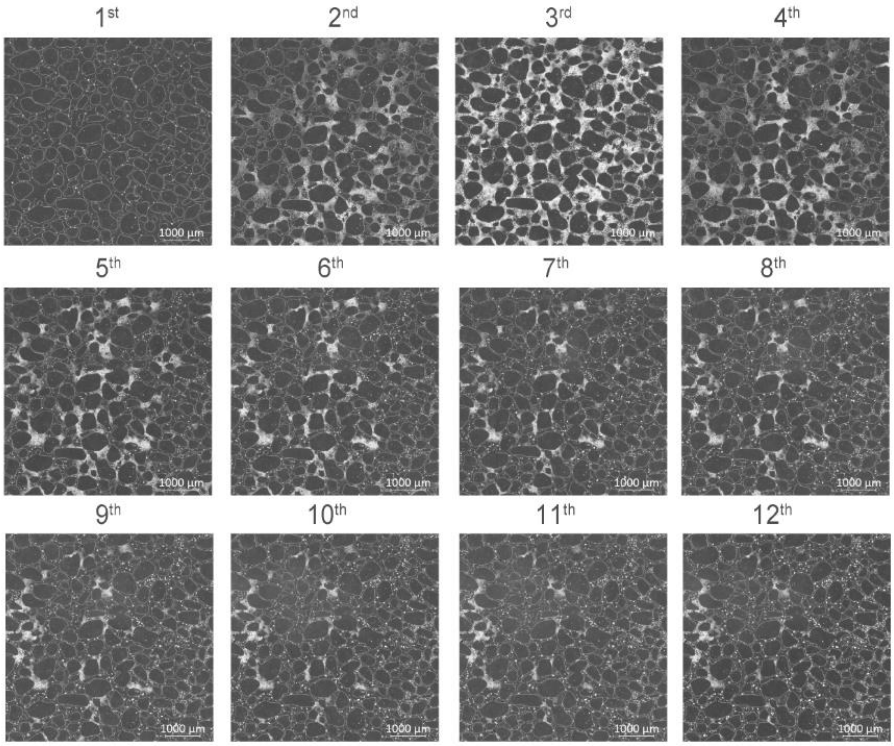

(a)

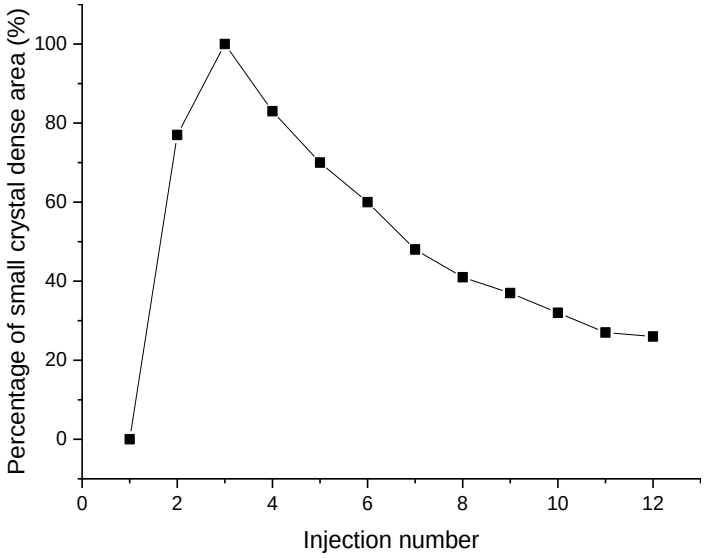

(b)

Figure 6 (a) Microscope images of microfluidic chip (protocol M2- the long injection protocol) at the completion of the injection interval of the 12 injections of cementation solution; (b) area percentage of small crystals plotted against injection numbers.

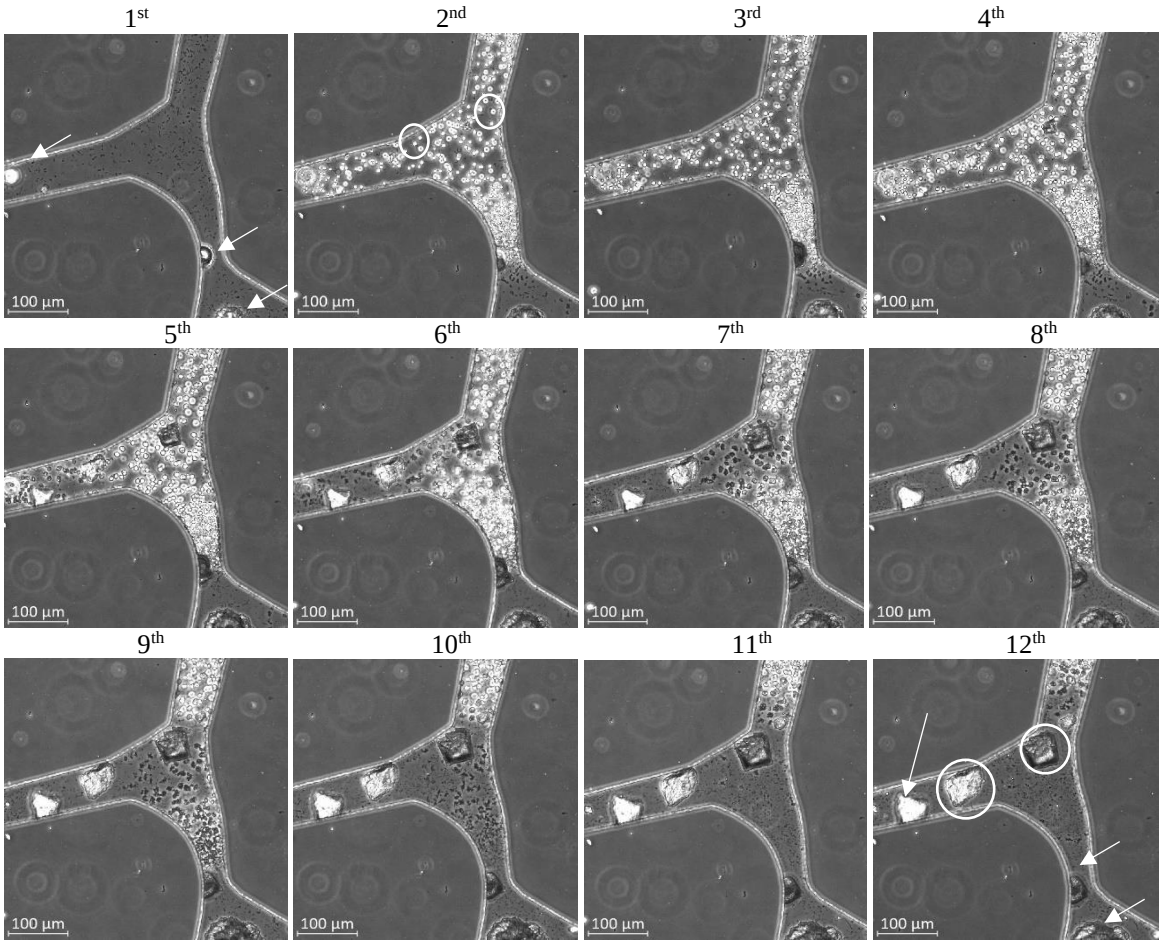

Figure 7 Images of a cell located at the centre of the 6 by 6 mm square taken after the completion of the injection inteveral of each cementation solution injection (long injection interval case)

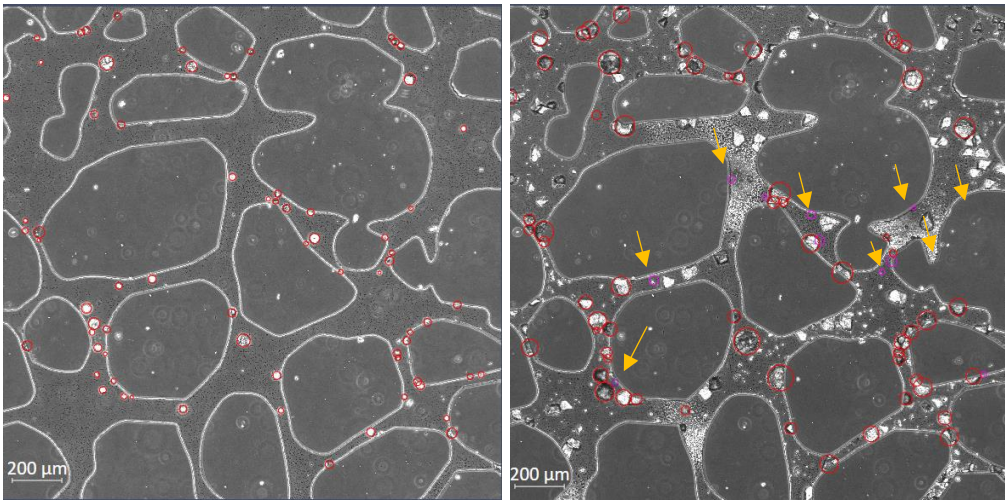

(a) (b)

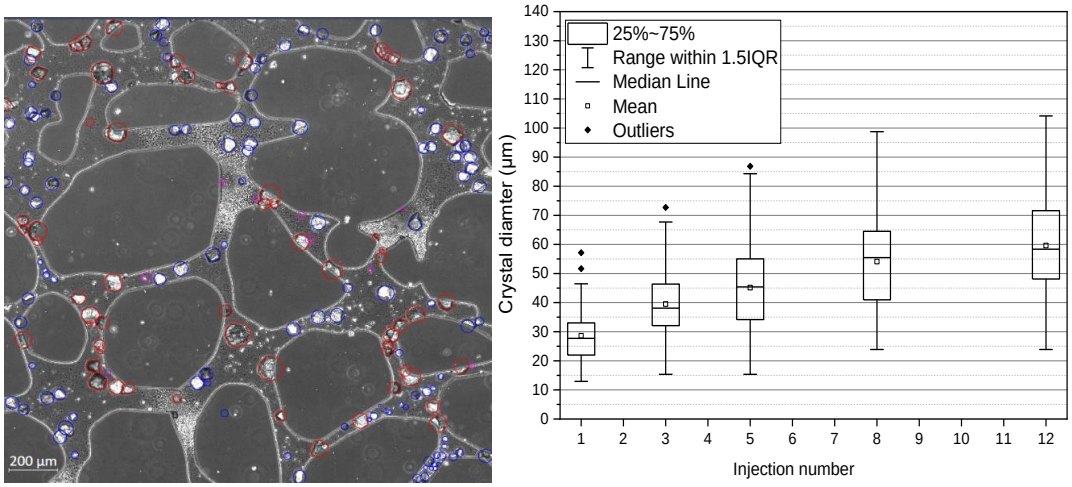

(c) (d)

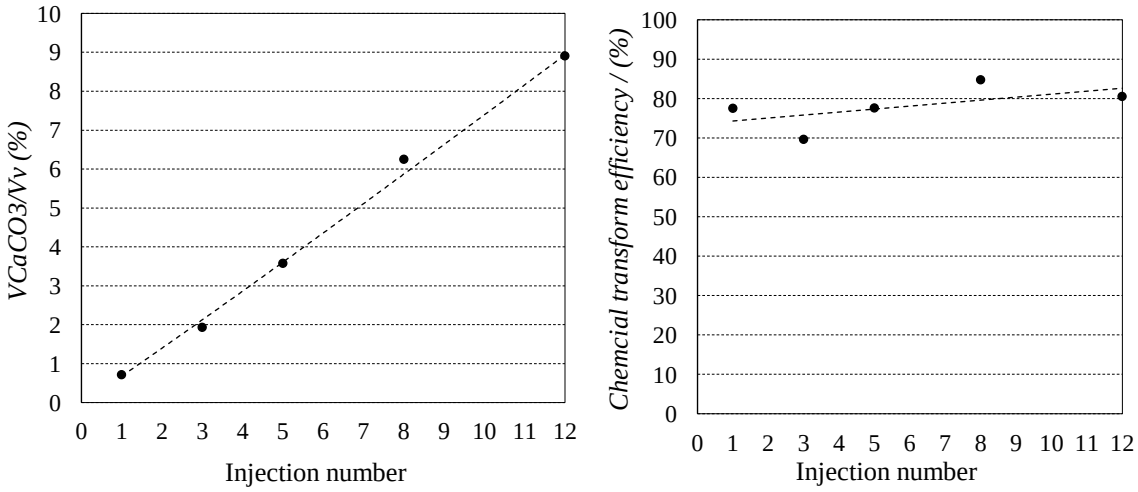

(e) (f)

Figure 8 Quantification of large crystals in the long injection protocol case. (a-b) Images at the centre of the microfluidic chip taken at the completion of injection interval after the first and the last injections of cementation solution. (c) images at the centre of the microfluidic chip taken at the completion of injection interval after the

last injections of cementation solution indicting the crystals started growing after the completion of the first injection;(d) box plots of the diameters of large crystals at completion of the injection intervals after the 1^{st}, 3^{rd}, 5^{th}, 8^{th} and 12^{th} injections. (e) voild ratio of large, small and all crystals (*Vc*) to the corresponding volume of the voids (V_v) in the 2 mm by 2 mm calculated zone after the 1^{st}, 3^{rd}, 5^{th}, 8^{th} and 12^{th} injections; (f) the chemical transformation efficiency calculated by the total volumn of only large crystals.

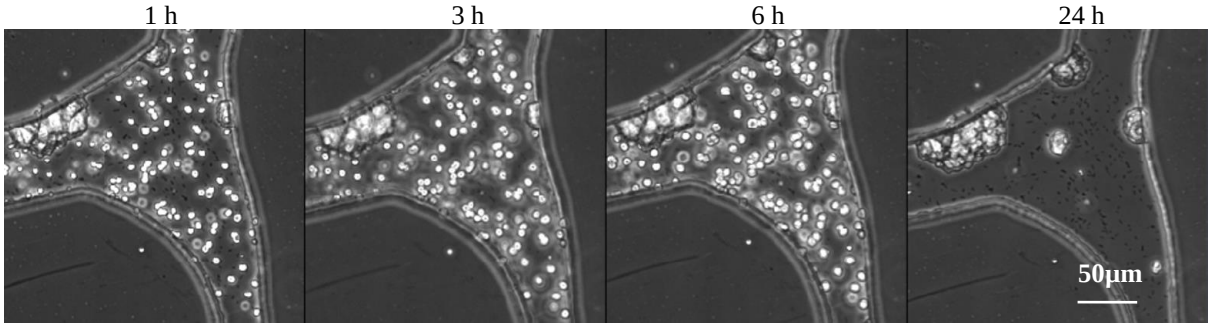

(a)

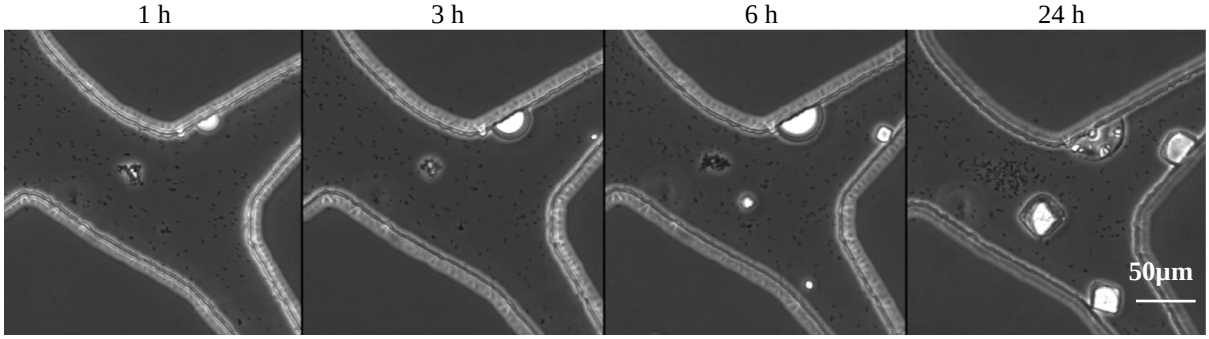

(b)

Figure 9 Microscope images of 250 μm by 250 μm square at one pore of microfluidic chips at 1, 3, 6 and 24 hours after the completion of the second injection of cementation solution (0.5 M) and first injection of cementation solution (1.0 M).

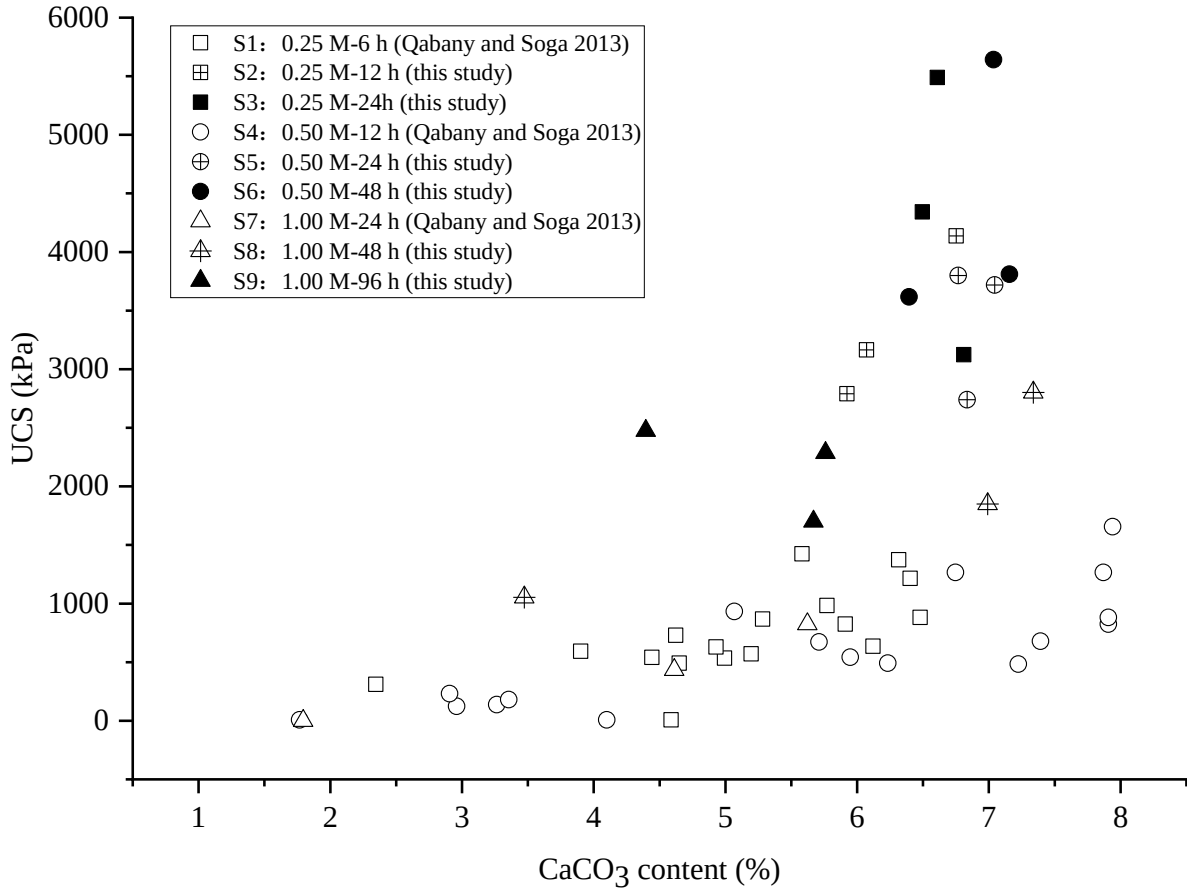

Figure10 $CaCO_3$ content v.s. UCS (comparison with the results of Al Qabany and Soga, 2013)

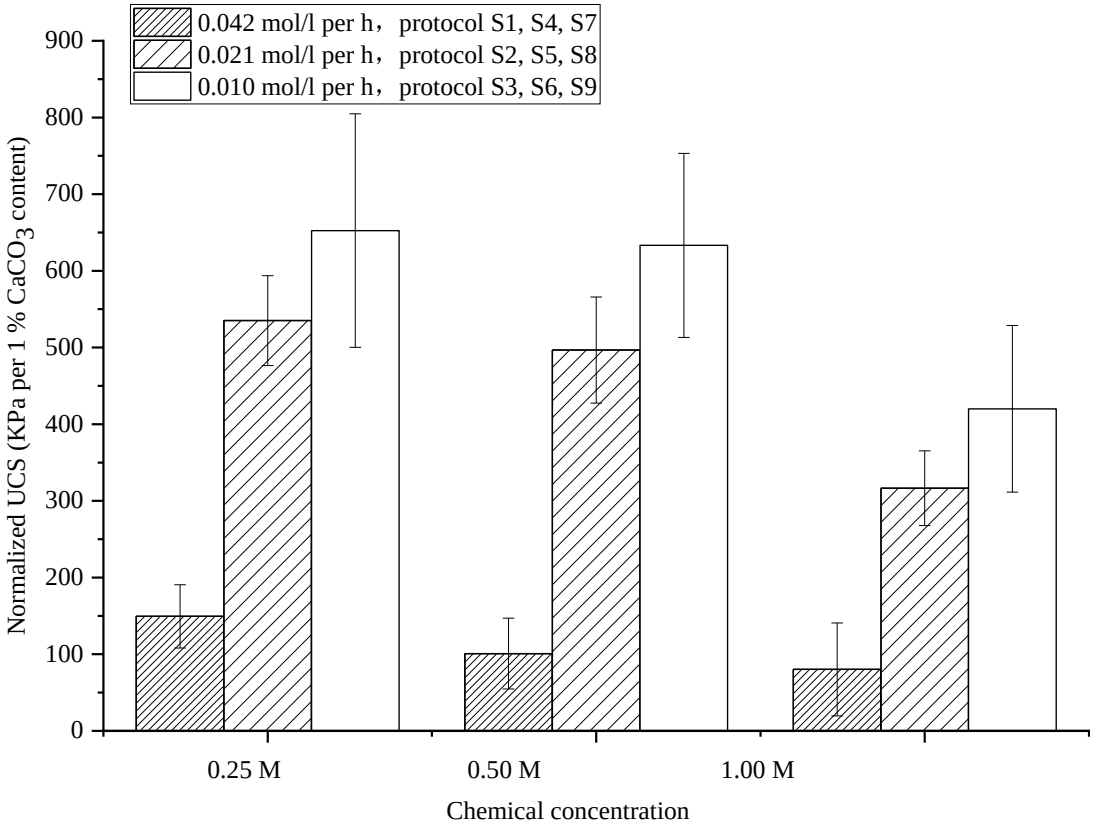

Figure 11. UCS values normalized by $CaCO_3$ content

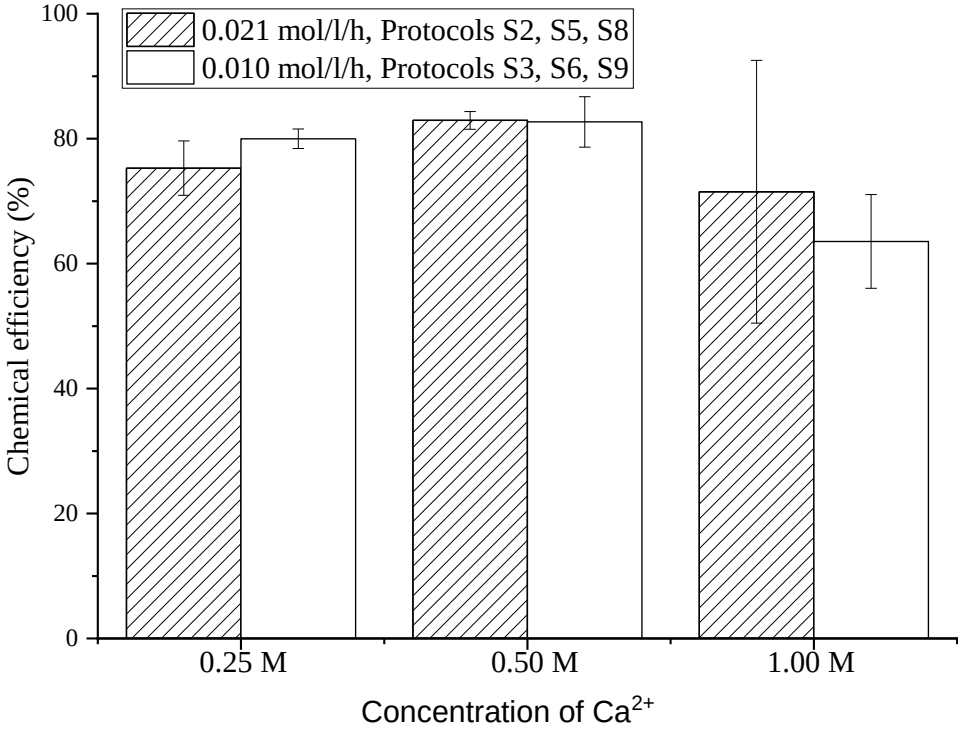

Figure 12. Chemical efficiencies of the MICP-treated sand samples. Data presented as mean ± standard error, n=3 (n is the number of times each treatment condition and the relative measurement was repeated)

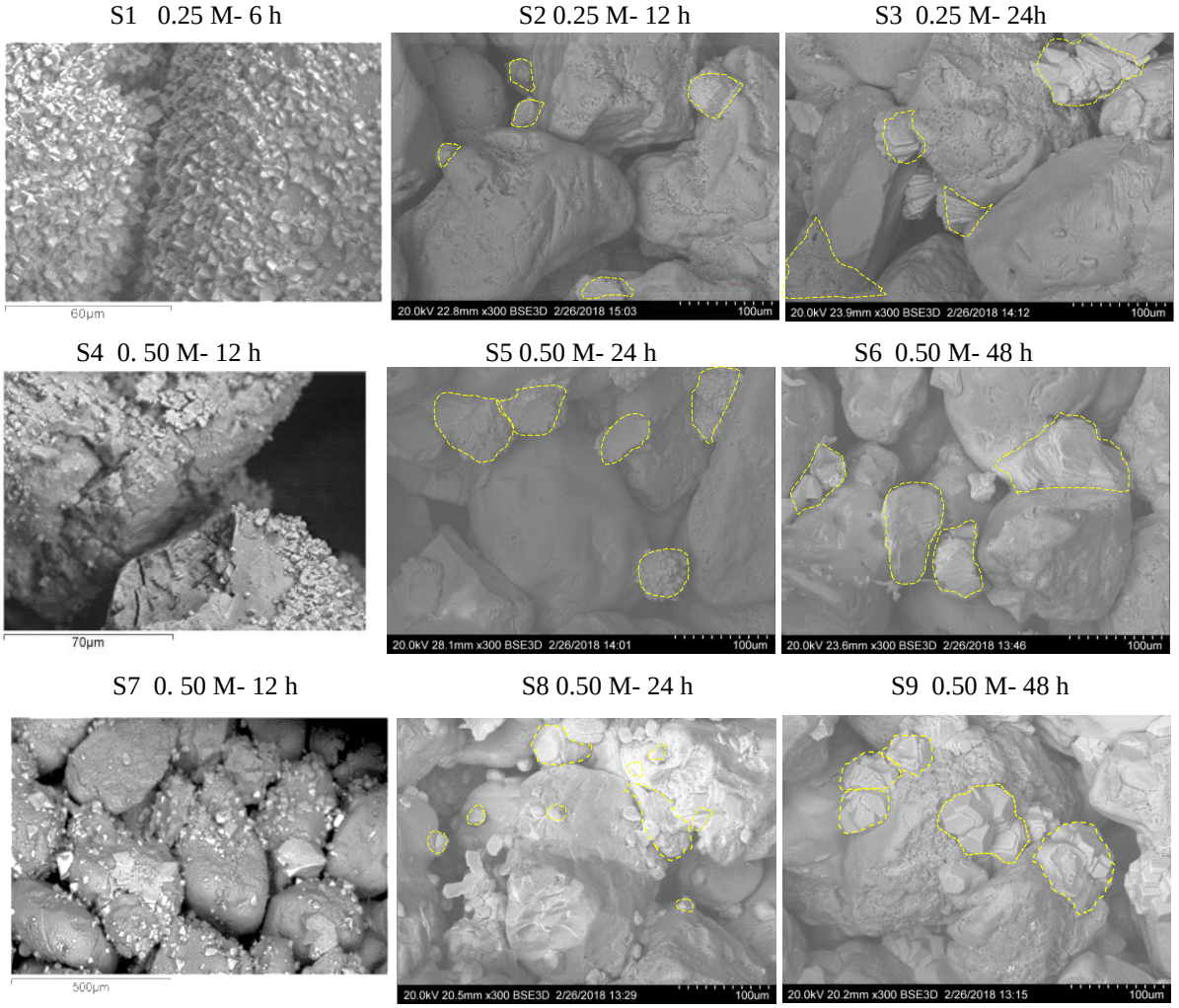

Figure 13. SEM images of $CaCO_3$ crystals inside MICP-treated sand samples after MICP treatments. (a) S1, 0.25 M-6 h injection interval treatment, $CaCO_3$ content is 4.8% (Al Qabany et al. 2012); (b) S2, 0.25 M-12 h injection interval treatment, $CaCO_3$ content is 6.1%; (c) S3, 0.25 M-24 h injection interval treatment, $CaCO_3$ content is 6.6%; (d) S4, 0.25 M-12 h injection interval treatment, $CaCO_3$ content is 6.0% (Al Qabany et al. 2012); (e) S5, 0.50 M-24 h injection intervaltreatment, $CaCO_3$ content is 7.0%; (f) S6, 0.50 M-48 h injection interval treatment , $CaCO_3$ content is 7.0%; (g) S7, 1.00 M-24 h injection interval treatment, $CaCO_3$ content is 3.9% (Al Qabany et al. 2012); (h) S8, 1.00 M-48 h injection interval treatment, $CaCO_3$ content is 7.0%; (i) S9, 1.00 M-96 h injection interval treatment, $CaCO_3$ content is 5.8%.

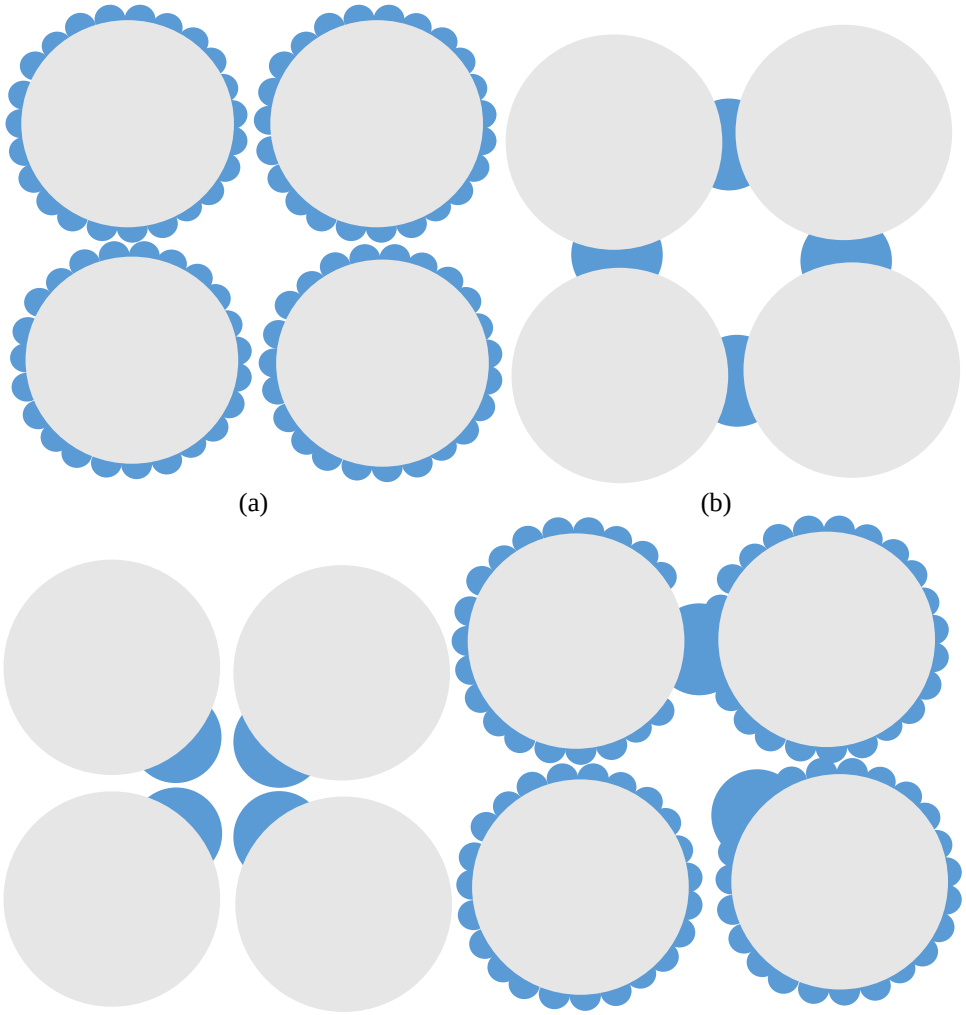

Figure 14. Schematic of $CaCO_3$ crystal precipitation pattern. (a) surface coating, (b) bonding, (c) pore filling, (d) mixtured pattern

981